ADVANCED MATERIALS
www.advmat.de

3D Spatiotemporal Mechanical Microenvironment: A Hydrogel-Based Platform for Guiding Stem Cell Fate

*Yufei Ma, Min Lin, Guoyou Huang, Yuhui Li, Shuqi Wang, Guiqin Bai, Tian Jian Lu, and Feng Xu**

Stem cells hold great promise for widespread biomedical applications, for which stem cell fate needs to be well tailored. Besides biochemical cues, accumulating evidence has demonstrated that spatiotemporal biophysical cues (especially mechanical cues) imposed by cell microenvironments also critically impact on the stem cell fate. As such, various biomaterials, especially hydrogels due to their tunable physicochemical properties and advanced fabrication approaches, are developed to spatiotemporally manipulate biophysical cues in vitro so as to recapitulate the 3D mechanical microenvironment where stem cells reside in vivo. Here, the main mechanical cues that stem cells experience in their native microenvironment are summarized. Then, recent advances in the design of hydrogel materials with spatiotemporally tunable mechanical properties for engineering 3D the spatiotemporal mechanical microenvironment of stem cells are highlighted. These in vitro engineered spatiotemporal mechanical microenvironments are crucial for guiding stem cell fate and their potential biomedical applications are subsequently discussed. Finally, the challenges and future perspectives are presented.

1. Introduction

Stem cells are undifferentiated cells with a capacity for self-renewal and differentiation into specialized cell lineages, which have found widespread applications in tissue engineering and regenerative medicine.[1] In these biomedical applications, it is important to spatiotemporally guide the fate of stem cells. Stem cell fate depends on the complex coeffect of their microenvironmental biochemical (e.g., soluble bioactive factors) and biophysical (e.g., structural organization and mechanical factors) cues.[2–6] Although the influence of biochemical cues has been intensively studied, accumulating evidence has indicated that biophysical cues (especially mechanical cues varying in a spatiotemporal manner) also have crucial impacts on guiding stem cell fate (e.g., differentiation).[7–10] For instance, stem cell differentiation can be directly regulated by the stiffness of the extracellular matrix (ECM), which is a highly dynamic structure constantly undergoing remodeling through deposition, degradation, or modification by surrounding cells.[11,12] Stem cells may sense and respond to the dynamic changes in ECM stiffness, and this dynamic feedback plays an important role in guiding stem cell fate.[11,13] Additionally, stem cells can respond to gradient stiffness in injured tissues and migrate directionally, which is vital to recruit cells for wound healing.[14] Besides ECM stiffness, some stem cells, especially those from musculoskeletal and cardiovascular tissues, experience dynamic mechanical

Dr. Y. Ma, Dr. M. Lin, Dr. G. Huang, Dr. Y. Li, Prof. F. Xu
The Key Laboratory of Biomedical Information Engineering of Ministry of Education
School of Life Science and Technology
Xi'an Jiaotong University
Xi'an 710049, P. R. China
E-mail: fengxu@mail.xjtu.edu.cn

Dr. Y. Ma, Dr. M. Lin, Dr. G. Huang, Dr. Y. Li, Prof. T. J. Lu, Prof. F. Xu
Bioinspired Engineering and Biomechanics Center (BEBC)
Xi'an Jiaotong University
Xi'an 710049, P. R. China

Prof. S. Wang
State Key Laboratory for Diagnosis and Treatment of Infectious Diseases
First Affiliated Hospital
College of Medicine
Zhejiang University
Hangzhou, Zhejiang Province 310003, P. R. China

Prof. S. Wang
Collaborative Innovation Center for Diagnosis and Treatment of Infectious Diseases
Hangzhou, Zhejiang Province 310003, P. R. China

Prof. S. Wang
Institute for Translational Medicine
Zhejiang University
Hangzhou, Zhejiang Province 310029, P. R. China

Dr. G. Bai
Department of Gynaecology and Obstetrics
First Hospital of Xi'an Jiaotong University
Xi'an 710061, P. R. China

Prof. T. J. Lu
MOE Key Laboratory for Multifunctional Materials and Structures
Xi'an Jiaotong University
Xi'an 710049, P. R. China

The ORCID identification number(s) for the author(s) of this article can be found under https://doi.org/10.1002/adma.201705911.

DOI: 10.1002/adma.201705911

loading (e.g., stress or strain) in vivo and respond to the applied mechanical stimulation.[15] Stem cells sense these mechanical cues and initiate intracellular biochemical responses via mechanotransduction pathways, which may play a crucial role in guiding their fate decision.[16,17] Thus, it is important to understand the roles of the spatiotemporal mechanical microenvironment in guiding stem cell fate.

Most existing studies on engineering the mechanical microenvironment of stem cells have been focused on 2D substrates. In a typical case, mesenchymal stem cells (MSCs) were seeded on polyacrylamide (PAA)-based substrates with different stiffness, resulting in the development of neurocytes, osteoblasts, and skeletal muscle cells on soft substrate (0.1–1 kPa), stiff substrate (>34 kPa) and substrate with intermediate stiffness (8–17 kPa), respectively.[18] However, 2D planar culture cannot recapitulate the native 3D cell microenvironment where stem cells reside, as reflected by the significantly different behaviors of stem cells in 2D and 3D mechanical microenvironments.[19] For instance, substrate stiffness affects cell morphology in 2D culture, and the changes in cell morphology are needed to direct MSC fate in response to substrate stiffness.[20–22] Comparably, MSC morphology does not depend on matrix stiffness during the osteogenic differentiation process when cells were encapsulated in 3D alginate hydrogels.[23] Depending on the matrix dimension, MSCs use different integrin receptors (e.g., α_v and α_5 integrins) to serve as RGD receptors when they are cultured in 2D and 3D matrices, respectively, with the same RGD density and stiffness.[23] Hence, the formation of mechanically mediated α_5-integrin–RGD bonds rather than MSC morphology is responsible for osteogenic differentiation in 3D.[23,24] Additionally, mechanical stress favors cardiac differentiation of cardiovascular progenitors encapsulated in 3D collagen hydrogels, whereas 2D conditions promote smooth muscle differentiation.[25] Hence, it is vital to evolve the study of stem cell fate in response to mechanical cues from 2D to 3D microenvironment.

To investigate stem cell behaviors in a 3D mechanical microenvironment, a variety of hydrogel-based culture models have been developed owing to the advantageous features of hydrogels, including excellent biocompatibility, high water content, and controllable physicochemical properties.[24,26] In particular, we have recently witnessed a great boom in nano/microengineering technologies, making it feasible to engineer 3D stem cell mechanical microenvironments in a spatiotemporal manner. For example, various strategies have been developed to construct heterogeneous mechanical microenvironments with gradient stiffness, such as controllable dipping of a matrix into a crosslinkable solution,[27] photopolymerization, or photodegradation with custom-designed masks (gradient darkening or sliding masks),[28,29] temperature gradients during the curing step[30] and a gradual freezing–thawing method.[31] Additionally, the cell mechanical microenvironment can be also dynamically controlled by softening or stiffening the microenvironment. For instance, tuning the hydrogel degradability[32] or forming a void in the hydrogel[7] can lead to hydrogel softening, whereas a repolymerization approach[33] and a sequential crosslinking strategy[34] have been reported to stiffen hydrogels. These approaches provide powerful tools to study how spatiotemporal mechanical cues influence stem cell behaviors in vitro.

Yufei Ma studied at the School of Materials Science and Engineering at Beijing University of Chemical Technology from 2005 to 2009, where she obtained a B.S. Afterward, she earned a Ph.D. in the School of Materials Science and Engineering at Tsinghua University, where she specialized in biomineralization and biomimetic materials. During 2016–2017, she worked as a research fellow at Harvard Medical School and VA Boston Healthcare System. She is now on the faculty of the School of Life Science and Technology at Xi'an Jiaotong University, where her research focuses on stem cell biomechanics and stem cell mechanical microenvironment engineering.

Min Lin achieved a B.S. degree in material science and engineering from Hefei University of Technology, China, and an M.S. degree in material science and engineering from Xi'an Jiaotong University, China. After completing his Ph.D. degree at the Bioinspired Engineering and Biomechanics Center at Xi'an Jiaotong University, he joined the faculty of Xi'an Jiaotong University and was subsequently promoted to associate professor. His current research is focused on biomechanics and mechanobiology of tissues and cells, and on bio- and nanomaterial synthesis for biomedical applications including photoresponsive cell microenvironments, gene/drug delivery, and point-of-care diagnosis.

Feng Xu received his Ph.D. in engineering from Cambridge University in 2008. During 2008–2011, he worked as a research fellow at Harvard Medical School and Harvard-MIT Health Science & Technology (HST). He founded the Bioinspired Engineering & Biomechanics Center with Prof. Tian Jian Lu in 2007. Currently, he is a full professor and associate dean at the School of Life Science and Technology, Xi'an Jiaotong University. His research aims at advancing human health through academic excellence in education and research that integrates engineering, science, biology, and medicine with a focus on biothermomechanics, engineering of the cell microenvironment, and point-of-care technologies.

Although many original articles and reviews have discussed stem cell microenvironments[35–37] or physical cues that stem cells experience,[4,38–40] most of these articles focused on the effect of physicochemical properties of the material on guiding stem cell fate and summarized studies on engineering uniform or static mechanical microenvironments. Recently, some articles have reviewed the progress on in vitro engineering dynamic cell microenvironments due to rapid development of reversible hydrogels and stimuli-responsive materials.[41–43] However, there is still a lack of a comprehensive review of the spatiotemporal changes in stem cell mechanical microenvironments both in vivo and in vitro, and their effects on stem cell fate. Therefore, here, we focus on the aspects of material design and engineering approach that can manipulate stem cell mechanical microenvironments in a spatiotemporal manner, which is a greatly promising area and is the major thrust of this review. In detail, we first describe the in vivo spatiotemporal mechanical microenvironment of some typical types of stem cells. We then systematically introduce recent advances in engineering 3D stem cell microenvironments with tunable mechanical cues in a spatiotemporal manner. These in vitro engineered spatiotemporal mechanical microenvironments are crucial for guiding stem cell fate, and their potential biomedical applications with focus on stem-cell-based therapy, pathological study, tissue engineering, and organoid formation are subsequently discussed. Finally, the challenges are highlighted to envision future perspectives. Our goals here are to encourage and inspire researchers to further understand this emerging field, to advance the development of novel biomaterials and strategies for engineering 3D stem cell microenvironments with spatiotemporally tunable mechanical cues, and to promote in vitro stem cell studies as well as their potential applications in vivo.

2. Native Spatiotemporal Mechanical Microenvironments of Stem Cells

The native stem cell microenvironment consists of stem cell-adhered supporting cells, soluble bioactive factors, and ECM that acts not only as supporting architecture but also as a container for cellular signaling biomolecules.[44] ECM comprises fibrous structural proteins (e.g., elastin and collagen), adhesive proteins (e.g., laminin, fibronectin, vitronectin), and polysaccharides in the form of glycosoaminoglycan (GAG) and proteoglycan, forming a complex 3D network. This network of fibrous structural proteins provides resident cells with mechanical resistance to tensile and shear stress, while polysaccharides are the water-absorbing components in the matrix due to their hydrophilic groups and consequently provide resident cells with resistance to compressive forces.[45] Adhesive proteins enable cell attachment to the matrix via specific receptors such as integrins, selectins and syndecan.[46] Integrins provide an essential link between the intracellular (e.g., cell cytoskeleton) and extracellular milieus and especially serve as crucial mechanotransducers, enabling cells to respond to the mechanical cues of surrounding matrices.[47]

In the native mechanical microenvironment, ECM, on the one hand, serves as a medium and transfers the external stress or strain to resident cells. On the other hand, the intrinsic mechanical property (e.g., stiffness) of the ECM is considered as an important mechanical cue in native mechanical microenvironment of stem cells. In detail, stem cells anchor onto ECM through focal adhesions formed via integrin clustering, and the mechanical links between the cellular cytoskeleton and focal adhesions allow the cells to generate cytoskeletal tensional states via a complicated traction force system.[45] Cytoskeletal tensional forces depend on the balance between intracellular actomyosin contractility and reaction forces exerted by the matrices, and the magnitude of the reaction forces depend on the matrix properties, including stiffness and topography etc. Cytoskeletal tensional forces are transmitted to the cell nucleus via intracellular pathways, and these mechanical cues are converted to biochemical responses that may affect stem cell fate.[40,48,49] In addition, extracellular forces (e.g., interstitial fluid-induced pressure and shear force) can also dynamically interact with cytoskeletal tensional forces and thus affect stem cell fate.[40] Hence, in the following paragraphs, we will elaborate on the native spatiotemporal mechanical microenvironments of some typical stem/progenitor cells.

Embryonic stem cells (ESCs) are able to differentiate into all somatic cells through the formation of embryoid bodies (EBs).[50,51] The spatial heterogeneity of mechanical forces within EBs can directly affect the differentiation of ESCs. Mechanical forces are generated within EBs in a 3D microenvironment when ESCs grow and differentiate. During the time course of differentiation, ESCs aggregate and EBs increase in size, leading to increased cytoskeletal traction force, which—in addition to gene regulation—possibly contributes to the initiation of differentiation programs. According to previous studies, when the anisotropy of cytoskeletal traction force is at a low level, ESCs develop into endoderm and mesoderm, in particular differentiating into neuronal,[52] cardiomyogenic,[53] and hematopoietic[54] lineages. In contrast, spatial cytoskeletal traction force at a high level of anisotropy mediates ectodermal cell lineage differentiation.[55]

MSCs are also one of the most studied stem cells for their high sensitivity to mechanical stimulation. MSCs can be obtained from various tissues, including placenta, umbilical cord, and adipose tissue, but are mainly obtained from bone marrow.[56] Physiologically, the mechanical microenvironment of bone marrow is known to be primarily affected by the dynamic shear stress that originates from intramedullary and interstitial fluid flow as well as the intramedullary compressive stress from the spatiotemporal loading of bones.[57] Therefore, such spatiotemporal variations in the mechanical microenvironment of bone marrow due to physiological activity or external stimulation may have significant effects on bone mesenchymal stem cell (BMSC) fate decisions.[58,59] Actually, accumulating evidence has shown that MSCs can respond to diverse dynamic mechanical forces (e.g., tensile stress,[60,61] compressive stress,[62,63] and shear stress[64,65]) and can be directed into specific differentiation pathways. For example, cyclic tensile stress can induce differentiation of MSCs toward a smooth muscle cell phenotype[66] or a myogenic phenotype,[67] whereas cyclic compressive loading can lead to upregulated expression of typical markers of chondrogenic differentiation.[62,68] Furthermore, dynamic shear stress derived from the interstitial flow in bone marrow is closely correlated with osteogenic differentiation.[69]

Besides, there are native spatiotemporal mechanical microenvironments of some other important stem/progenitor cells including endothelial progenitor cells (EPCs), valvular interstitial cells (VICs), and tendon-derived stem cells (TDSCs) etc., which play crucial roles in maintaining physiological functions of cells. For instance, EPCs are mobilized form bone marrow to peripheral blood. During this process, they experience the shear stress originated from dynamical blood flow and tissue fluid flow, which induces EPC differentiation into mature endothelial cells and thus contributes to angiogenesis in tissues.[70] VICs are the most common cell type in heart valves, and their matrix mechanics is regarded as a crucial controller of VIC phenotype.[33,71] VICs in the matrices with normal elastic modulus are quiescent fibroblasts.[72] When the matrix mechanics changes abnormally, VICs can be activated to myofibroblasts, exhibiting strong proliferation, cytokine secretion, and matrix remodeling, which leads to valve disease.[33,71,73] In addition, TDSCs reside within the tendon tissue, which intersperse among collagen fiber bundles and align along the long axis of tendon tissue.[74] It is widely accepted that TDSCs undergo similar mechanical microenvironments as the whole tendon tissues. As mechanical load-bearing tissues, tendons play a vital role in the musculoskeletal system by transferring tensile loads from muscle to bone to stabilize joints and achieve joint motions. Hence, TDSCs are always subjected to a complicated dynamic mechanical microenvironment (both stretching and compressive loading), with a tensile force more prevalent during joint movement.[75] TDSCs are mechanoresponsive and alter their biological behaviors in response to the mechanical loading conditions.[76] It has been reported that appropriate mechanical loading (less than 8% strain) can induce differentiation of TDSCs into tenocytes and support their normal biological functions, while a large mechanical loading (8% strain) directs TDSCs to nontenocyte lineages differentiation (adipocytes, chondrocytes, and osteocytes), which leads to tendon pathological change.[77,78] Additionally, the mechanical microenvironment of TDSCs in tendon is not uniform. The region of bone tendon is stiffer than mid substance of the tendon, which has been confirmed in a human Achilles tendon model.[79]

In addition, in vivo spatiotemporal mechanical microenvironment may significantly influence wound healing and disease progression by guiding migration and regulating differentiation of stem cells. For example, MSCs can egress from bone marrow, migrate through tissue, and home in on an injury site.[80] To direct such migration, local injured tissue often shows mechanical heterogeneity (e.g., stiffness gradient). It serves as a homing signal that encourages MSCs to preferentially accumulate, while chemical signals are commonly implicated. Hence, such a stiffness gradient in injured tissue may guide MSC migration (denoted as durotaxis) to ensure that the right cells can differentiate in the right place as part of the wound healing process.[18,81–83] In addition, damage occurring in cardiac tissues activates the differentiation of cardiac fibroblasts to myofibroblasts, where the differentiated myofibroblasts secrete and excessively accumulate ECM leading to ECM stiffening.[84] The stiffened ECM may further accelerate cardiac myofibroblast differentiation by enhancing TGF-β1 activation through the AT_1R pathway, resulting in continuous cardiac fibrosis development.[84–86]

3. Mechanical Properties of Hydrogels for 3D Stem Cell Culture In Vitro

To recapitulate stem cell behaviors in both physiological and pathological conditions, engineering 3D spatiotemporal mechanical microenvironments in vitro may help researchers to understand how these particular mechanical cues affect stem cell fate. In recent, hydrogels mimicking native ECM have been developed and tailored for 3D stem cell culture in vitro.[87–89] Most studies have investigated the effects of linear elasticity of 3D hydrogels on stem cell fates, which have been extended to nonlinear elasticity and even more recently to viscoelasticity of hydrogels. Furthermore, spatial and temporal modulation of mechanical properties has also been performed to engineer heterogeneous or dynamic stem cell mechanical microenvironments to mimic the spatiotemporal mechanical alterations in native ECM. Therefore, the mechanical property of hydrogels is a significant aspect of their capability to fulfill the requirements of engineering 3D spatiotemporal mechanical microenvironments of stem cells.

3.1. Linear Elasticity

Linear elasticity is characterized by a constant Young's modulus or stiffness that doesn't change along with the applied stress or strain, which is the commonly studied mechanical property of hydrogels in cell mechanical microenvironment engineering. The stiffness of hydrogels can usually be controlled by the molecular weight of polymers, polymer concentration, and crosslinking degree.[90–92] Hence, hydrogels with tunable stiffness in a wide range are ideal for engineering 3D cell mechanical microenvironments.[93,94] For example, the stiffness of softest hydrogel (99.95% water) for 3D stem cell culture is only ≈0.1 kPa, while the stiffest cell culture hydrogel system has a stiffness of up to ≈200 kPa.[13,45] It has been confirmed that the hydrogel with suitable stiffness may support stem cell proliferation, main its self-renewal, and even induce stem cell differentiation to specific cell lineage.[30,38,80,87,90,95–99] For example, human ESCs in hyaluronic acid (HA)-based hydrogels of 0.35 kPa[98] and rat neural stem cells (rNSCs) in gelatin-based hydrogels ranging from 1.2 to 3.6 kPa[99] could proliferate well at their undifferentiated state. In addition, softer hydrogels are in favor of differentiation into cell lineages from soft tissues (e.g., brain, fat, and muscle), while stiffer hydrogels are beneficial to differentiation into cell lineages from hard tissues (e.g., cartilage and precalcified bone). As a typical example, murine MSCs encapsulated in alginate hydrogels exhibited adipogenesis and osteogenesis preferably at 2.5–5 kPa and 11–30 kPa, respectively. Similar results were also observed in RGD-modified agarose or poly(ethylene glycol) (PEG) hydrogels.[23] Besides, some other stem/progenitor cell differentiation into various cell lineages or maintaining their self-renewal in response to hydrogel stiffness in 3D microenvironments are particularly illustrated in **Figure 1**A. It is found that both differentiation of stem cells into various cell lineages and maintenance of self-renewal need specific a mechanical microenvironment with appropriate stiffness ranges, though it may differ depending on the type of stem cells.

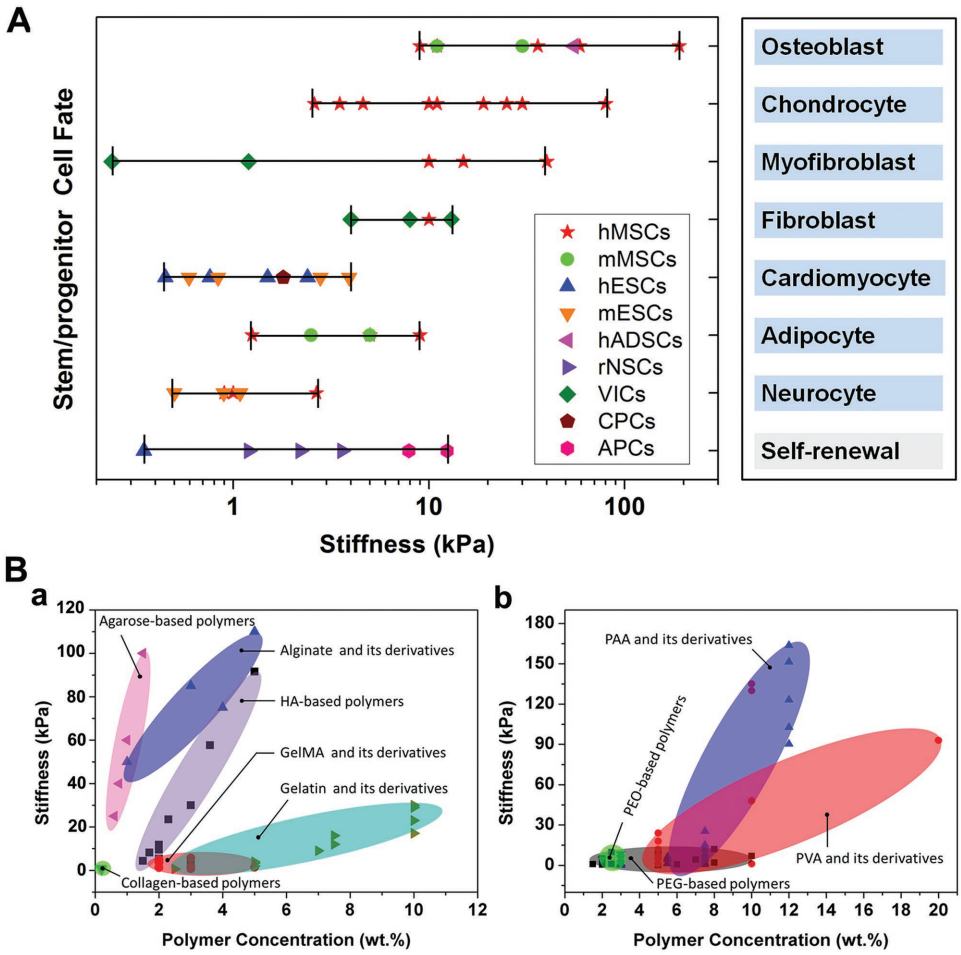

Figure 1. The relationship between stem/progenitor cell fate decision and the engineered 3D mechanical microenvironments in vitro. A) Stem/progenitor cell fate decision in 3D hydrogel microenvironments with specific mechanical properties. (hMSCs: human mesenchymal stem cells; mMSCs: murine mesenchymal stem cells, hESCs: human embryonic stem cells; mESCs: murine embryonic stem cells; hADSCs: human adipose-derived stem cells; rNSCs: rat neural stem cells; VICs: valvular interstitial cell; CPCs: cardiomyocyte progenitor cells; APCs: adipose progenitor cells). B) Material selection diagram: hydrogel stiffness plotted against polymer concentration. Ashby plots describe the possible stiffness ranges of both a) naturally derived and b) synthetic hydrogels. The diagram is helpful to provide design guidelines in material selection of polymer hydrogels for engineering 3D mechanical microenvironments of stem cells.[7,31,33,90,96,100–111]

Hydrogels derived from natural polymers including protein-based (e.g., collagen, gelatin, and silk fibroin etc.) and polysaccharide-based (e.g., HA, agarose, and alginate etc.) polymers are often mechanically weak and with limited control over their mechanical properties. For example, the stiffness of self-assembled collagen hydrogel is only ≈1 kPa, which gradually decreases due to uncontrollable degradation. Various approaches have been developed to improve the stability and mechanical properties of these naturally derived hydrogels by incorporating functional groups (e.g., tryamine,[90] thiolate,[112] and acrylate[113]) and/or adding other components (e.g., gelatin methacrylate (GelMA)/PEG,[114] HA/PEG,[87] or collagen/PAA[115]). In addition, different covalent crosslinking strategies have also been applied. For instance, Choi and Kim[116] increased the stiffness of an alginate/PAA hydrogel via remodeling through secondary crosslinking of the polymeric networks in a defined polymer composition.

Compared to naturally derived hydrogels, synthetic polymers such as PEG, PAA, poly(ethylene oxide) (PEO), poly(vinyl alcohol) (PVA), and their derivatives have also been utilized to fabricate hydrogels for engineering 3D mechanical microenvironments of stem cells in vitro.[37,117–119] For these synthetic hydrogels, bioactive molecules, including ECM-derived peptides, protein fragments and growth factors, can be readily incorporated via functional termini (e.g., hydroxyl, carboxyl, and amino) to improve their biocompatibility.[119,120] In addition, synthetic hydrogels allow rational design of mechanical properties (e.g., stiffness) through a well-defined polymer chain composition without arousing the immunogenicity-related concerns that are associated with some naturally derived hydrogels.[38]

It is well known that the stiffness of most naturally derived hydrogels can be efficiently mediated by changing polymer concentration. For example, the stiffness of agarose-based hydrogels sensitively responds to the polymer concentration, which increases from ≈20 to 100 kPa within a narrow range of polymer concentration (Figure 1B-a). In contrast, it seems

that the stiffness of some synthetic hydrogel, for example, PEG-based hydrogel doesn't strongly depend on the polymer concentration, where the variation in hydrogel stiffness is only several kilopascals when the polymer concentration increases from ≈1% to ≈10% (Figure 1B-b). In Figure 1B, the Ashby plots summarize the stiffness ranges of both naturally derived and synthetic hydrogels commonly used for engineering 3D stem cell mechanical microenvironments in vitro.

3.2. Nonlinear Elasticity

Certain intracellular and extracellular filamentous biopolymer hydrogels, including F-actin, collagen, fibrin, and vimentin, are known to exhibit nonlinear elasticity as reflected by stress stiffening behavior.[121,122] When stress increases beyond a critical stress (σ_c), stiffness increases along with the increase in the applied stress. Such a nonlinear mechanical behavior has been confirmed to have a great influence on maintaining tissue integrity, mechanical homeostasis, and wound healing.[9,123] It has been reported that the nonlinear elasticity of hydrogels may affect the modes of cell migration[124,125] and regulate differentiation of stem cells in 3D microenvironments.[9] For instance, human foreskin fibroblasts cultured in nonlinear elastic collagen hydrogels exhibited lamellipodia-based migration, as compared to lobopodia-based migration in linear elastic cell-derived matrices.[124,126] Additionally, polyisocyanopeptide (PIC)-based hydrogels exhibited a series of tunable stress stiffening behaviors, and human MSCs encapsulated in these hydrogels differentiated from adipogenic to osteogenic lineages when the stress stiffening behaviors varied.[9]

3.3. Viscoelasticity

In addition to elasticity, most hydrogels, especially biopolymer-based hydrogels, show both elastic and viscous properties.[127,128] These hydrogels are viscoelastic and often exhibit stress relaxation (e.g., a decrease in stress in response to constant applied strain) or creep (e.g., an increase in strain in response to constantly applied stress) behaviors. The viscous characteristics of hydrogels may be attributed to various dissipative events such as the unbinding of weak bonds, polymer disentanglement, protein unfolding, and molecule slipping. There are several factors that influence the viscoelasticity of hydrogels, including polymer molecular weight or network chain length,[129,130] crosslink type and density,[131] hydrogel composition or concentration,[132] and degradation.[133] Recent evidences have indicated that hydrogel viscoelasticity significantly affects cell spreading, proliferation and differentiation. For example, Mooney and co-workers reported that spreading and proliferation of fibroblasts on alginate-based elastic substrates decreased as compared with that on viscoelastic substrates with the same initial modulus.[134] Moreover, they found osteogenic differentiation of murine MSCs was enhanced in viscoelastic hydrogels with faster stress relaxation.[10] Therefore, hydrogel viscoelasticity should be considered when engineering 3D mechanical microenvironment of stem cells.

3.4. Other Mechanical Properties

Some other mechanical properties (e.g., strength) of hydrogels should also be considered. Strength represents the ability to withstand an applied stress without failure. For example, to mimic the mechanical microenvironment of stem cells in cartilage or tendon, high mechanical strength is required to ensure hydrogel functions without fracturing. Several types of hydrogels with high strength have been developed based on various principles. For instance, double-network (DS) hydrogels have been produced via interpenetrating short or long chain polymers. When DS hydrogels are formed at low polymer concentrations (more than 90% water), the elastic modulus is still as high as ≈190 kPa, while compressive strength can reach up to ≈10 MPa, similar to the mechanical properties of natural articular cartilage.[135] Alternatively, homogeneous network hydrogels, such as slide ring hydrogels and tetra-arm polymer hydrogels, have also been developed to realize high stretchability due to their particular structural features.[136] Additionally, nanocomposite hydrogels with inorganic agents (e.g., carbon nanotubes,[137] graphene oxide,[138] or clay[139]) added to the network can effectively achieve high strength. Future studies are still needed to explore the potential applications of these hydrogels in engineering 3D mechanical microenvironments.

3.5. Hydrogel Material–Stem Cell Interactions in 3D

The interactions between stem cells and materials are fundamental to stem cell behaviors including cell migration, differentiation, and self-renewal. As an important factor of the cell biophysical environment, mechanical properties of materials can largely affect stem cell behaviors at both spatial and time scales.[140] Various proteins such as integrins, actin cytoskeleton, nuclear lamins, and YAP/TAZ transcription coactivators, have been found to mediate matrix stiffness-regulated stem cell behaviors.[140,141] A recent interesting work found that when cultured on hydrogels with heterogeneous stiffness (minimal matrix models of scars), MSCs exhibited less cell-to-cell noise of scar-like phenotypes than those cultured on homogeneously stiff hydrogels.[142] It was found that NKX2.5 (a strong SMA repressor) slowly exited the nucleus of cells cultured on rigid hydrogel substrates, which could contribute to bulk-average responses. It was also demonstrated that mechanosensitive proteins of MSCs, including myosin-IIB, lamin-A and SMA, responded to matrix stiffness at different timescales.[142] Further work is needed to verify the above findings in 3D.

On the other hand, several excellent recent studies found that MSCs showed mechanical memory when sequentially cultured in microenvironments of different stiffness.[143,144] Specifically, the differentiation and fibrogenesis of MSCs were dependent on previous culture time, seeming that MSCs remember their past mechanical microenvironments. Such behaviors were regulated by intracellular mechanical rheostats such as YAP/TAZ,[143] NKX2.5,[142] and microRNA-21,[144] where YAP/TAZ and NKX2.5 were shown to regulate short-term mechanical memory and microRNA-21 was shown to regulate long-term mechanical memory. Based on the these findings, soft priming of MSCs before cell transplantation has been found to benefit

MSC therapy in tissue repair.[144] Considering that stem cells in vivo usually experience dynamically changed mechanical microenvironments, it will be of particular interest to further investigate stem cell mechanical memory in native-like 3D cell microenvironments.

Most hydrogels used to mimic the cell microenvironment are typically elastic, while many natural extracellular matrices are viscoelastic and the interactions between stem cells and viscoelastic materials have been seldom investigated. With the development of advanced viscoelastic materials and models, the principles and mechanisms underlying cell–viscoelastic material interactions are uncovering.[145–147] A recent representative work demonstrated that faster matrix stress relaxation promoted MSC spreading, proliferation, and osteogenic differentiation through adhesion-ligand binding, RGD ligand clustering, actomyosin contractility, and YAP nuclear localization.[148] It was suggested that matrix stress relaxation could account for the effect of matrix degradation on stem cell behaviors, considering that MSCs in peptide-functionalized PEG hydrogels were found to proteolytically degrade the matrices and locally convert them from mechanically elastic to viscoelastic forms.[133] Shenoy and coworkers[145] combined experimental and theoretical approaches and tested different cell types (human MSCs, 3T3 fibroblasts, U2OS osteosarcoma line), and found that cell spreading was independent of viscosity on stiff substrates, while an optimal level of viscosity on soft substrates maximized cell spreading. Besides viscosity, the ECM usually undergo nonreversible plastic deformation (cells can also show mechanical plasticity[149]) under external mechanical loading or cell-induced remodeling, which may also contribute to regulate stem cell behaviors.[150]

Recently, Heilshorn and co-workers demonstrated that the stemness maintenance of neural progenitor cell was influenced by matrix remodeling but not correlated with initial hydrogel stiffness.[151] Within elastin-like protein hydrogels, stemness was maintained independent of cytoskeletal tension generation and ligand clustering, but relying on hydrogel degradation. They employed two additional material systems: physically remodelable alginate hydrogels and proteolytically degradable PEG hydrogels, to test the generality of their findings. The results showed that matrix remodeling regulated cadherin-mediated cell–cell contact to maintain the stemness of neural progenitor cell. It is worth noting that N-cadherin adhesive interactions have also been found to modulate MSC perception of the matrix mechanical properties.[152] These results indicate that matrix remodeling ability and cell–cell contact are important design parameters for engineering stem cell microenvironments.

4. Engineering 3D Spatiotemporal Mechanical Microenvironments of Stem Cells In Vitro

A variety of polymers, such as naturally derived polymers and synthetic polymers, have been fabricated into hydrogels for engineering mechanical microenvironments in vitro (**Table 1**). Generally, there are two primary types of mechanical cues that cells experience from hydrogels, including: i) hydrogel stiffness or elasticity (intrinsic mechanical cue) and ii) stress/strain applied to hydrogels (extrinsic mechanical cue). In the following section, we will describe the existing strategies for

Table 1. Overview of commonly used polymer hydrogels for engineering mechanical microenvironments in vitro.

Polymers	Strategies	Mechanical characteristics	Spatiotemporal modulation	Applications	Refs.
Methacrylated alginate	Dual-crosslinking (calcium- and UV- crosslinking)	Stiffness patterns (checkerboard, island, and strip)	Spatial	Cell alignment Complex tissue engineering	[153]
PEG monoacrylate (PEGA)	Photodegradation	Stiffness patterns (regular or random; different stiff-to-soft ratios)	Spatial	Stem cell fate decision Mechanotransduction study	[154]
PAA	Controlled hydrogel thickness based on topographically defined substrates	Stiffness patterns	Spatial	Mechanotactic cell migration Tissue engineering	[155]
Matrigel	Matrigel–glass interface; hydrogel–substrate edge effects	Stiffness gradients (Stiffness at the Matrigel–glass interface is as a function of gel height.)	Spatial	Mechanobiology study	[156]
PEG dimethacrylate (PEGDM)	Mixing two polymer solutions via a gradient maker	Stiffness gradients (≈12–306 kPa)	Spatial	Graded osteogenesis Mineralized tissue gradient	[157]
Collagen and alginate	Microfluidics	Softer core/stiffer shell structure	Spatial	Ovarian microtissue engineering	[158]
PVA/HA	Freezing–thawing method	Stiffness gradients (≈20–200 kPa)	Spatial	Stem cell differentiation Tissue regeneration	[31]
MeMaHA	Michael-type addition reaction and proteolytic degradation	Dynamic softening	Temporal	Stem-cell-based therapy	[32]
Alginate dialdehyde/alginate	Void formation due to hydrolysis	Dynamic softening (from 110 to 5 kPa)	Temporal	Bone regeneration Stem-cell-based therapy	[7]

Table 1. Continued.

Polymers	Strategies	Mechanical characteristics	Spatiotemporal modulation	Applications	Refs.
MeHA	Step-wise crosslinking	Dynamic stiffening	Temporal	Tissue development Wound healing	[34]
Thiolated-HA (SH-HA)	Crosslinking with PEG diacrylate (PEGDA) with controlled molecular weight	Dynamic stiffening (from 1.9 to 8.2 kPa)	Temporal	Cardiomyocyte maturation Cardiac tissue engineering	[112]
PEG-norbornene (PEG-NB)	Repolymerization	Dynamic stiffening (from 0.24 to 1.2 kPa or 13 kPa)	Temporal	Pathological study of the fibrotic diseases	[33]
PEG-NB	Tyrosinase-mediated oxidation reaction	Dynamic stiffening	Temporal	Mimicking the process of tumor development	[159]
Collagen/alginate	Ionic crosslinking or decrosslinking	Reversible stiffening or softening	Temporal	Cell–ECM interaction study	[88]
DNA oligomer–PAA	DNA oligomer crosslinking or decrosslinking	Reversible stiffening or softening	Temporal	Pathological study of the cancer Tissue engineering	[160]
SH-PVA, PEG-allylether and β-cyclodextrin-allylether	Supramolecular "host–guest" interactions	Reversible stiffening or softening	Temporal	Cell fate study	[161]
PDPA–PMPC–PDPA triblock copolymer	pH response	Reversible stiffening or softening	Temporal	Dynamic cell adhesion–detachment manipulation	[162]
PHPMA–PNIPAAm	Temperature response	Reversible stiffening or softening	Temporal	Systematic stem cell research	[163]
Cys-P_4-Cys artificial protein	Protein topological entanglement	Reversible stiffening or softening	Temporal	Mimicking the native tissues	[164]
Polyprotein GB1-R-(GB1-GL5CC-I27-R)$_2$	Ru^{2+}-mediated photocrosslinking; Redox controlled protein folding–unfolding switch	Reversible stiffening or softening (oxidizing condition: 40 kPa; reducing condition: 10 kPa)	Temporal	Tissue engineering	[165]
HPMA/AKtm/DTT	Substrate–enzyme (adenylate kinase, ATP) interaction; Substrate-recognition-mediated conformational change	Reversible stiffening or softening	Temporal	ECM dynamics capture	[166]
PEG-NB	Diaphragm pump and pressure regulator	Dynamic stretching	Temporal	Stem cell differentiation Tissue engineering	[167]
GelMA	Polymerization in designed trapezoidal molds	Tensile stain gradients (linear, parabolic, and exponential gradients)	Spatial	Mechanobiology study Complex tissue engineering	[168]
GelMA	Microfluidics	Compressive stain gradients (from ≈65% to ≈15%)	Spatial	Cellular alignment Tissue engineering	[169]
Agarose	Custom bioreactor	Dynamic compression	Temporal	Chondrogenesis Cartilage tissue engineering	[170]
Alginate	Tubular perfusion system	Dynamic compression and shear	Temporal	Chondrogenesis Cartilage tissue engineering	[171]
Polyisocyanopeptide	Warming above ≈15 °C to form the hydrogel	Stress stiffening (critical stress: from ≈9 to 19 Pa)	Temporal	Stem cell differentiation Mechanotransduction study	[9]
P(NIPAAm-*r*-CA)-*b*-PEO-*b*-P(NIPAAm-*r*-CA)	Physical crosslinking	Viscoelasticity	Temporal	Mechanobiology study	[172]
PEG	Covalent crosslinking with hydrazone	Viscoelasticity	Temporal	Mechanobiology study	[173]
Alginate	Ionic crosslinking; Changing of molecular weight and cross-linking density; coupling of short PEG spacers to the polymer chains	Viscoelasticity Tunable stress relaxation ($\tau_{1/2}$: from ≈1 h to ≈1 min)	Temporal	Cell–ECM interaction study Mechanotransduction study Bone tissue engineering	[10]

Table 1. Continued.

Polymers	Strategies	Mechanical characteristics	Spatiotemporal modulation	Applications	Refs.
WW domain (CC43 or Nedd4.3 variant)-based block copolymer, proline peptide-based block copolymer	Mixing-induced molecular recognition crosslinking; Design of the frequency of repeated association domains per chain and the binding strength between association domains	Viscoelasticity	Temporal	Clinical cell encapsulation applications Stem-cell-based therapy	[174]
Tax-interactive protein-1 modified triangular trimetric CutA protein (CutA-TIP1), PDZ-peptide-PEG	Shear stress-dependent reversibility of association/decoupling of protein–peptide-specific interaction	Dynamic viscoelasticity $\omega < 0.8$ rad s^{-1}, viscoelasticity; $\omega > 0.8$ rad s^{-1}, viscosity	Temporal	Cartilage tissue engineering	[175]

engineering 3D mechanical microenvironments (e.g., linear elastic, nonlinear elastic and viscoelastic microenvironments) of stem cells, and especially advanced fabrication approaches that can spatiotemporally manipulate mechanical cues (e.g., spatially heterogeneous or temporally dynamic mechanical cues) in 3D stem cell microenvironments in vitro (**Figure 2**).

4.1. Engineering 3D Spatiotemporal Stiffness Microenvironments of Stem Cells

Matrix stiffness is the most common mechanical cue that stem cells experience within the ECM,[17] and it is also an important mechanical cue that affects stem cell behaviors (e.g., cell spreading and differentiation). However, another opinion believes that protein tethering on ECM instead of stiffness is essential cue to guide stem cell fate. To resolve this disagreement, Ding and co-workers developed a well-defined surface patterning technique based on RGD nanopatterned PEG hydrogels to decouple the effects of matrix stiffness and surface chemistry, and illustrated undoubtedly that matrix stiffness was a potent regulator of stem cell fate.[176,177] In the following section, we mainly focus on the effects of various spatiotemporal stiffness cues in 3D on guiding stem cell fate.

4.1.1. Engineering Spatially Nonuniform Stiffness Microenvironments

Many native tissues are mechanically heterogeneous, such as calcific vascular tissues, fibrocartilage, and heart valves.[178–180] Mechanical heterogeneity in terms of patterned stiffness or even gradient stiffness has a remarkable impact on guiding stem cell migration and differentiation, which plays important roles in embryonic development, wound healing and disease progression.[181] To mimic the patterned stiffness of native tissues in vitro, a photopatterning method has been widely used to fabricate photocrosslinkable hydrogels with a spatially patterned stiffness through custom-designed photomasks.[153,182,183] For example, methacrylated alginate was used to prepare dual ionic and photocrosslinked hydrogels, and the checkerboard, island and strip stiffness patterns were created by using different photomasks to achieve precise spatial control over regions that were only calcium-crosslinked versus dual-crosslinked (**Figure 3**A).[153] Similarly, photodegradable hydrogels combined with a photopatterning method is an alternative strategy to achieve stiffness patterns. Anseth and co-workers[154] reported a photodegradable hydrogel through copolymerizing a photodegradable PEG diacrylate (PEGdiPDA) with PEGA. The photolabile crosslinker contained two nitrobenzyl ether groups that could be cleaved

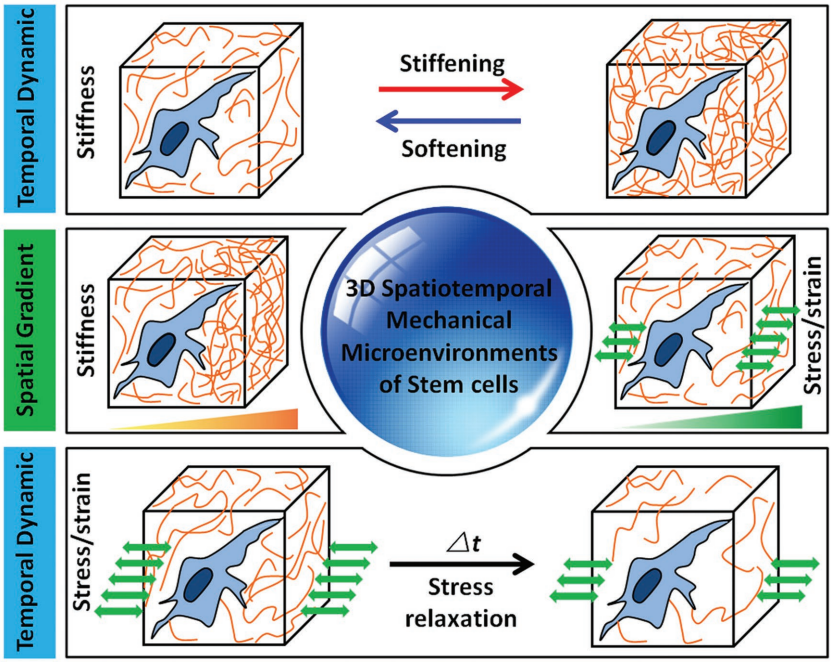

Figure 2. Engineering 3D spatiotemporal mechanical microenvironments of stem cells in vitro. Hydrogel stiffness and the applied mechanical stimulation such as stress/strain are regarded as intrinsic and extrinsic mechanical cues, respectively. Particularly, some of these mechanical cues exist in a spatiotemporal manner, including spatial gradient (e.g., gradient stiffness or stress/strain) and temporal dynamics (e.g., mechanical stiffening or softening, stress relaxation).

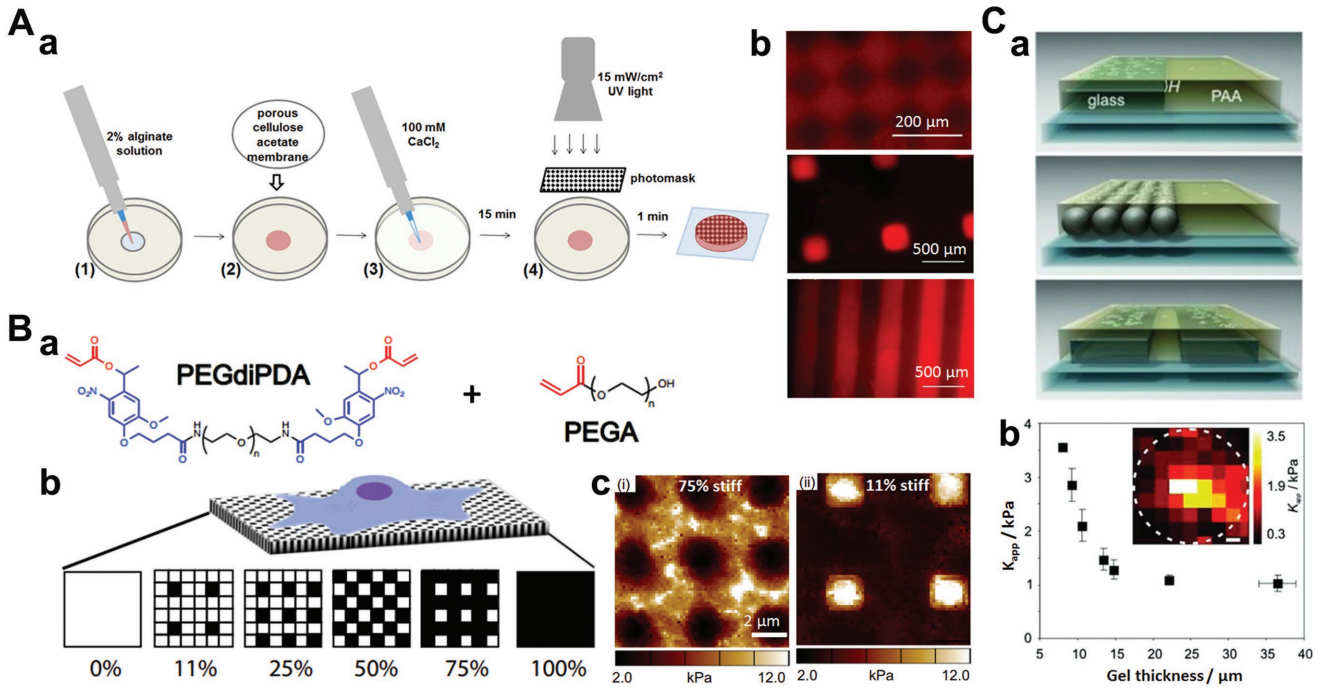

Figure 3. Engineering patterned stiffness microenvironments in vitro. A) Dual-crosslinked hydrogel-based stiffness patterns. a) Schematic of dual-crosslinked hydrogel fabrication. Calcium-crosslinked hydrogels are prepared using only steps 1–3. Hydrogels with patterned stiffness required the use of a photomask and UV light in step 4. b) Fluorescence photomicrographs using methacrylated rhodamine to show stiffness patterns. A) Reproduced with permission.[153] Copyright 2015, American Chemical Society. B) Photodegradable hydrogel-based stiffness patterns. a) Chemical structures of the photodegradable crosslinker (PEGdiPDA) and PEGA. Acrylate functional groups are labeled in red and the photodegradable nitrobenyzl ether is labeled in blue. b) An illustration of hMSCs on patterned stiffness hydrogels with different stiff-to-soft ratios. Black indicates chrome-covered areas that will remain stiff, and white squares indicate areas exposed. c) AFM elastic moduli maps of two stiffness patterns. B) Reproduced with permission.[154] Copyright 2016, National Academy of Sciences. C) Topographically patterned glass substrate-based stiffness patterns. a) Schematic of different designed substrates to generate stiffness patterns by variation in PAA hydrogel height. b) Apparent stiffness K_{app} of a "bead substrate," determined by AFM indentation experiments, as a function of gel thickness. Inset: apparent stiffness distribution of the substrate over a bead; the bead is indicated by the white broken line. Scale bar: 10 µm. C) Reproduced with permission.[155] Copyright 2012, Wiley-VCH.

upon irradiation, resulting in the release of PEG and thereby the decrease of hydrogel stiffness in situ. Such PEG-based photodegradable hydrogels with regular or random stiffness patterns and different stiff-to-soft ratios were fabricated via several designed photomasks (Figure 3B). It was observed that cell morphology and Yes-associated protein (YAP) activation of hMSCs were highly associated with stiffness pattern organization and stiff-to-soft ratios in these hydrogels. In addition, to generate more complex stiffness patterns, PAA hydrogels with controlled thickness were polymerized on three different topographically defined glass substrates, i.e., "step substrates," "bead substrates," and "groove substrates" (Figure 3C).[155] For each kind of glass substrates, the distance between the hydrogel surface and the underlying glass surface varied according to the structure of the topographically patterned glass substrate, leading to a local change in the height of the superficial hydrogel and thus apparent stiffness patterns.

Besides patterned stiffness, several approaches have also been developed to generate gradient stiffness in vitro. For example, a gradient maker equipped with mixing and stock chambers that loading PEGDM solutions with different concentrations was used to achieve PEGDM hydrogel-based cell microenvironments with gradient stiffness ranging from 12 to 306 kPa (**Figure 4**A).[157] Additionally, microfluidics is another commonly used method to fabricate hydrogel particles or fibers with heterogeneous mechanical properties by varying polymer composition and concentration.[158,184,185] For example, a non-planar microfluidic flow-focusing device was developed for 3D culturing of early secondary preantral follicles using a collagen core (softer) and an alginate shell (stiffer) to mimic medulla and cortex, respectively (Figure 4B).[158] This mechanically heterogeneous microenvironment was found to enhance follicle development and ovulation. However, these approaches involve complex fabrication procedures or devices, which are considered as obstacles and need to be overcome. To construct gradient stiffness microenvironment with a facile fabrication procedure, a PVA/HA hydrogel with gradient stiffness (≈20–200 kPa) was generated using a liquid nitrogen (LN_2)-contacting gradual freezing-thawing method to engineer a gradient stiffness microenvironment (Figure 4C).[31] When the PVA/HA aqueous solution contacted the LN_2 surface, the bottom side (LN_2-contacted side) of the solution froze rapidly, and then the solution gradually froze along the longitudinal direction to the top side during the freezing step, leading to a gradient stiffness in PVA/HA hydrogels. It was found that hBMSCs preferred stiffness ranges for differentiation into specific cell lineages, e.g., ≈20 kPa for nerve cells, ≈40 kPa for muscle cells, ≈80 kPa for chondrocytes, and ≈190 kPa for osteoblasts.

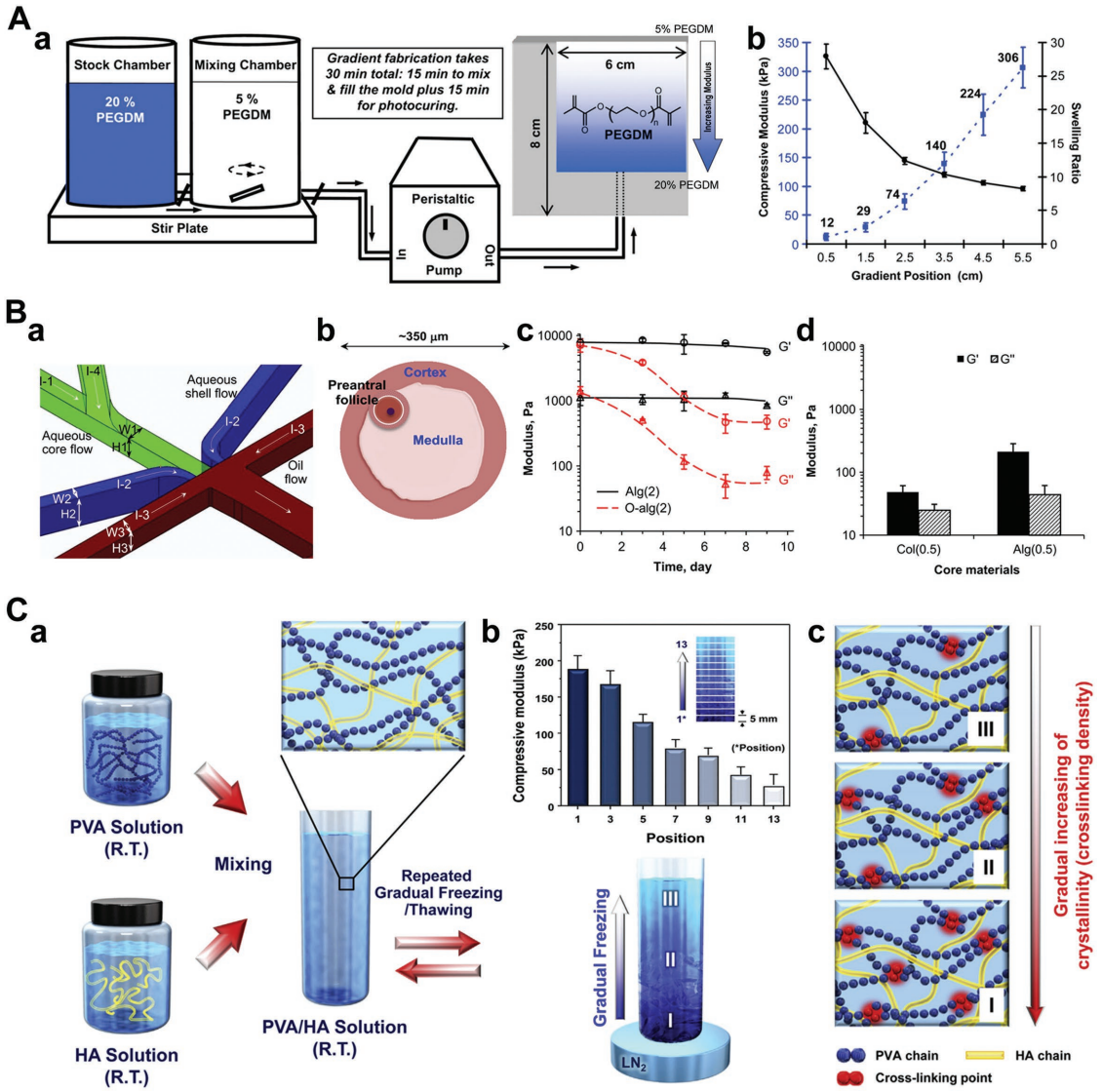

Figure 4. Engineering gradient stiffness microenvironments in vitro. A) Stiffness gradients produced by a gradient maker. a) Schematic illustration of the combinatorial platform used to prepare PEGDM hydrogels with gradient stiffness. b) The compressive modulus (dotted blue line) and swelling ratio (solid black line) are plotted for the hydrogel at different positions along the gradient. A) Reproduced with permission.[157] Copyright 2010, Elsevier. B) Stiffness gradients produced by a microfluidics method. a) Schematic view of the non-planar design of the flow-focusing junction. b) Schematic illustration of the in vitro engineered microenvironment of preantral follicles to mimic ovarian microtissue. c) The storage (G') and loss (G'') moduli of two different harder hydrogels, 2% alginate [Alg(2)] and 2% alginate with oxidization [O-alg(2)] for making the shell (cortex). d) The two moduli of two different softer hydrogels, 0.5% alginate [Alg(0.5)] and 0.5% collagen [Col(0.5)] for making the core (medulla). B) Reproduced with permission.[158] Copyright 2014, Elsevier. C) Stiffness gradients produced by a liquid nitrogen-contacting gradual freezing–thawing method. a) Schematic diagrams showing the fabrication procedures. b) Compressive modulus of the PVA/HA hydrogel sections along the longitudinal direction. c) Mechanism of the formation of PVA/HA hydrogel with stiffness gradients. The creation of a stiffness gradient in the PVA/HA hydrogel can be explained by the arisen gradient of freezing temperature and time along the longitudinal direction during the freezing step. C) Reproduced with permission.[31] Copyright 2016, Elsevier.

4.1.2. Engineering Dynamic Stiffness Microenvironments

The native cell mechanical microenvironment may dynamically change with time, either soften or stiffen, during tissue development, regeneration and pathological processes.[34] Therefore, hydrogels with static stiffness cannot fully represent the dynamic mechanical cues in many native cell microenvironments. To overcome this limitation, hydrogels with dynamic mechanical properties have been developed to mimic mechanical softening or stiffening processes. A typical softening system commonly used for engineering 3D dynamic mechanical microenvironments is based on biodegradable hydrogels.[186] The encapsulated cells can regulate the degradation process of these cell-laden biodegradable hydrogels. However, this process is challenging to control. Recently, modification of polymer chains in hydrogels with enzymatically degradable units (e.g., matrix metalloproteinase (MMP)-degradable peptides) in combination with a sequential

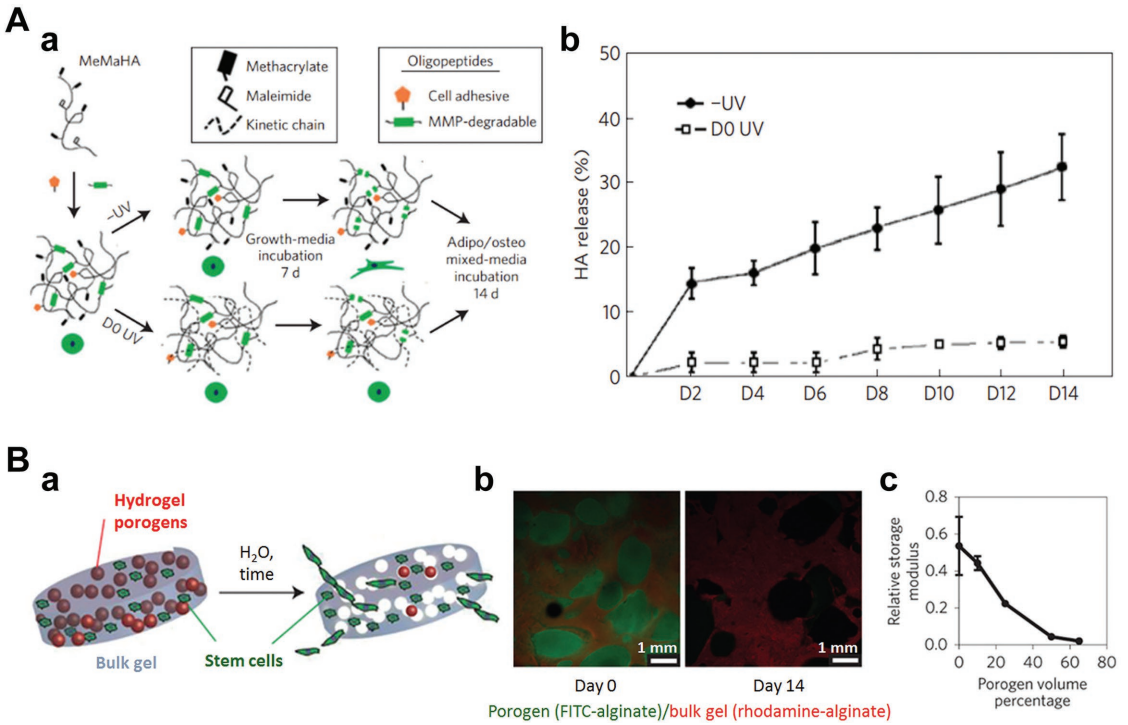

Figure 5. Engineering 3D mechanical softening microenvironments in vitro. A) Hydrogel softening via tuning the degradability. a) Schematic of sequential crosslinking of MeMaHA using a primary addition and secondary radical polymerization to create UV and D0 UV hydrogels, respectively. b) Degradation of -UV and D0 UV hydrogels. For all time points, the percentage of HA release was greater from UV than D0 UV hydrogels. A) Reproduced with permission.[32] Copyright 2013, Nature Publishing Group. B) Hydrogel softening via forming the void. a) Schematic diagram of the strategy to create void-forming hydrogels. Porogens (red) and stem cells (green) are coencapsulated into a bulk hydrogel (gray). Pores (white) form within the hydrogel due to porogen degradation. b) Confocal micrographs of FITC-labeled porogens (green) within a rhodamine-labeled bulk hydrogel (red). c) Relative shear modulus G' of void-forming hydrogels as a function of volume fraction of porogen. Values of G' are normalized to the value obtained for a standard hydrogel (without porogen) at day 1. B) Reproduced with permission.[7] Copyright 2015, Nature Publishing Group.

crosslinking approach has been used to temporally mediate hydrogel stiffness by tuning the degradability (**Figure 5**A).[32] For instance, both methacrylate (Me) and maleimide (Ma) groups were incorporated into HA polymer chains and then the modified HA (MeMaHA) was subjected to multiple crosslinking steps to form UV hydrogels and D0 UV hydrogels, respectively. UV hydrogels rapidly released HA due to proteolytic degradation, while D0 UV hydrogels released little HA because of the newly formed kinetic chains, resulting in controlled dynamic softening of hydrogels. Alternatively, addition of a hydrolysable component into hydrogels can also decrease mechanical stiffness dynamically (Figure 5B).[7] Alginate dialdehyde-based microspheres (as the hydrolysable porogens) were incorporated into "bulk" alginate hydrogels and then degraded due to hydrolysis, leading to the formation of hydrogels with many voids. Importantly, the porogen degradation effectively controlled the void formation and subsequent stiffness variation (from 110 to 5 kPa) in hydrogels. Rheological analysis indicated that the void-forming hydrogels exhibited a porogen density-dependent decrease in shear modulus. Finally, it was confirmed that void-forming hydrogels with a stiffness of 60 kPa could best regulate the osteogenesis of the encapsulated MSCs.

In addition to ECM softening, stiffening is another dynamic change in ECM mechanical properties that cells may encounter in vivo. ECM stiffening may be induced by cell contraction or matrix overdeposition, which plays an important role in tissue development, fibrosis formation and tumor progression.[112,187–189] Hence, a variety of hydrogels have been combined with novel strategies to mimic ECM stiffening in 3D. For instance, Mabry and Lawrence[33] developed PEG-based hydrogels with dynamic stiffening properties to study the phenotype change of VICs in a 3D microenvironment (**Figure 6**A). Eight-arm PEG-NB was polymerized with adhesive peptide and MMP-degradable crosslinking peptide using lithium phenyl-2,4,6-trimethylbenzoylphosphinate (LAP) as a photoinitiator. VICs were encapsulated in this PEG-based hydrogel (with a stiffness of 0.24 kPa) and allowed to spread post encapsulation. Then, the cell-laden hydrogels were immersed and swollen in the mixture of 8-arm PEG-NB, 8-arm PEG-thiol (PEGSH) and LAP solutions, and subsequently repolymerized in situ to increase the hydrogel modulus to 1.2 and 13 kPa, respectively. In another example, 8-arm PEG-NB and a peptide linker with additional tyrosine residues were used to prepare cell-laden hydrogels that can be in situ stiffened by a tyrosinase-mediated reaction (Figure 6B).[159] More specifically, the primary hydrogels were synthesized by a light-mediated thiol-norbornene polymerization of 8-arm PEG-NB and bis-cysteine-bis-tyrosinebearing peptide crosslinkers. The pendant tyrosine residues in primary hydrogels could be oxidated in the presence of tyrosinase into dihydroxyphenylalanine (DOPA), DOPA quinone, and finally into DOPA dimer, leading to additional crosslinks and thus stiffening the cell-laden hydrogels in 3D.

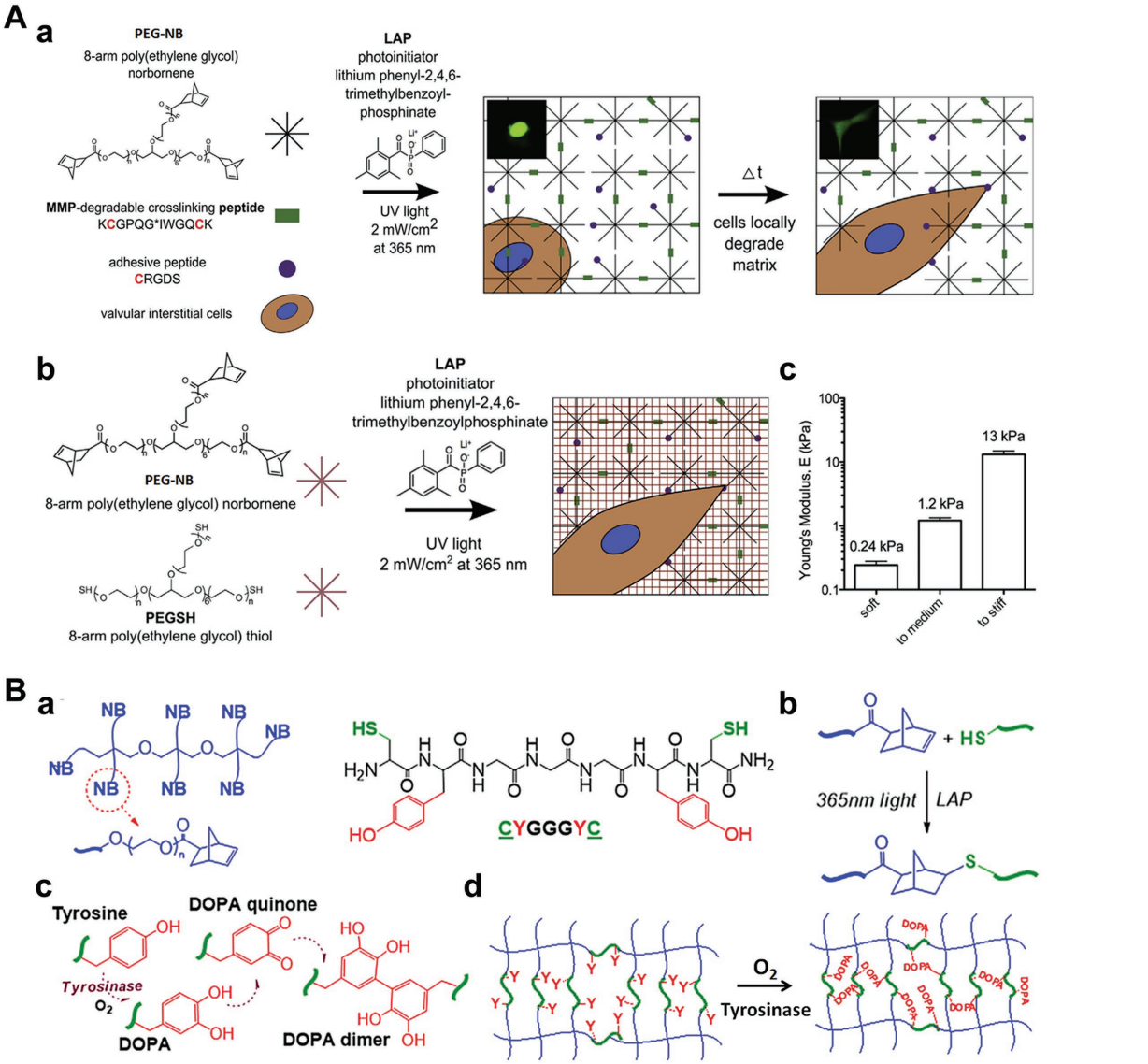

Figure 6. Engineering 3D mechanical stiffening microenvironments in vitro. A) Hydrogel stiffening via a light-mediated repolymerization. a) Schematic of VIC encapsulation and b) stiffening the cell-laden hydrogel. c) Young's modulus (*E*) of soft and stiffened hydrogels. A) Reproduced with permission.[33] Copyright 2015, Elsevier. B) Hydrogel stiffening via an enzyme-mediated repolymerization. a) Structure of 8-arm PEG-NB and model bis-cysteine-bis-tyrosine peptide crosslinker CYGGGYC. b) Light mediated thiol-norbornene photoclick reaction to form primary PEG-based hydrogels. c) Tyrosinase-mediated oxidation of tyrosine into DOPA, DOPA quinone, and DOPA dimer. d) Schematic of tyrosinase-mediated DOPA dimer formation in PEG-based hydrogels. B) Reproduced with permission.[159] Copyright 2016, Elsevier.

Besides nonreversible mechanical softening or stiffening, two strategies have also been developed to engineer 3D mechanically reversible microenvironments, including a) addition of the chemical reagents to crosslink or decrosslink the hydrogels; and b) preparation of the stimulus-responsive hydrogels to achieve crosslinking or decrosslinking of the hydrogels. For the first strategy, a collagen/alginate hydrogel system was created by Gillette et al.[88] In this system, collagen was first self-assembled as a stable structural network. By introducing Ca^{2+} or sodium citrate, alginate (acting as a modulatory element) could be switched between crosslinked and decrosslinked states, achieving reversible mechanical stiffening or softening of collagen/alginate hydrogels (**Figure 7**A). In addition, DNA-crosslinked PAA hydrogels were fabricated to reversibly switch their mechanical properties by adding or removing a DNA oligomer crosslinker (Figure 7B).[160] Noncomplementary DNA oligomer sequences with 5′ acrydite modifications (SA1 and SA2) were copolymerized with acrylamide groups in PAA polymer chains, leading to the formation of SA1 and SA2 polymers. When a DNA oligomer "linker" (L2) containing a sequence complementary to SA1, a sequence complementary to SA2 and a "toehold'' sequence was introduced, it hybridized with SA1 and SA2 polymers, forming stiffer PAA-based hydrogels. Once another DNA oligomer sequence (R2) complementary to L2 was added, PAA-based hydrogels hybridized with the "toehold" to unzip L2

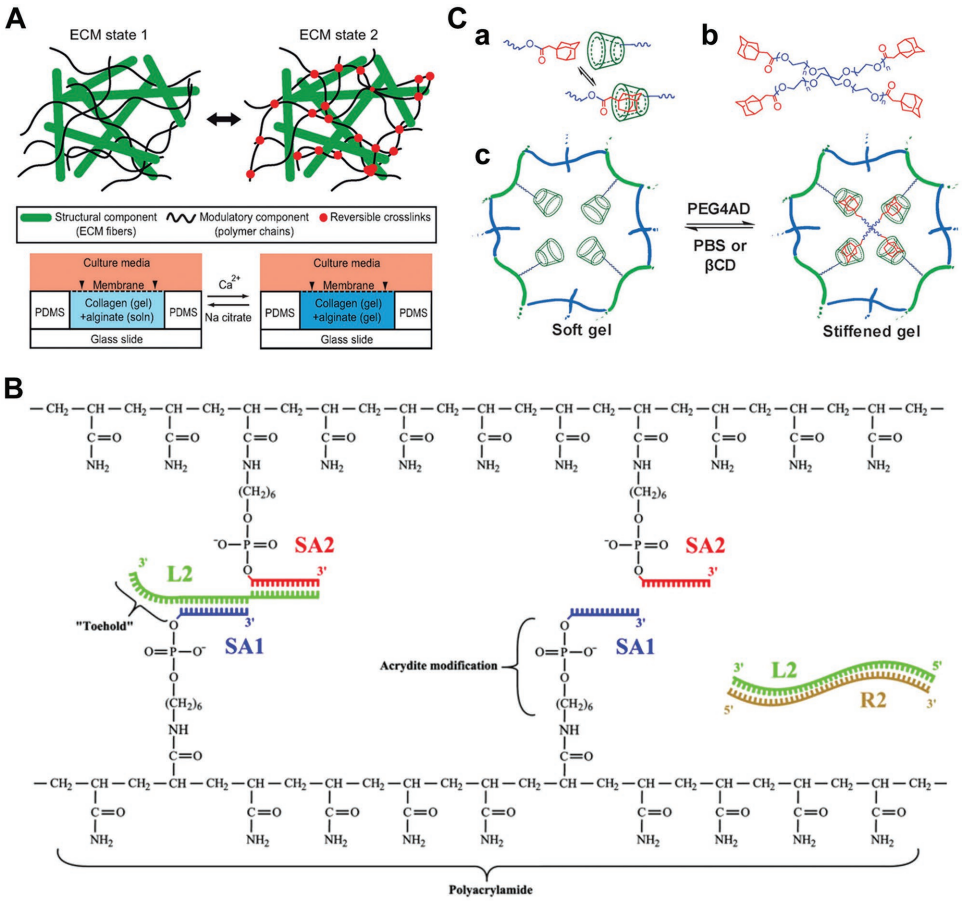

Figure 7. Engineering 3D mechanically reversible microenvironments in vitro using the first strategy. Three different mechanically reversible microenvironments were engineered based on A) Ca^{2+}-crosslinked collagen–alginate hydrogels, A) Reproduced with permission.[88] Copyright 2010, Wiley-VCH. B) DNA-crosslinked PAA hydrogels Reproduced with permission.[160] Copyright 2011, Biomedical Engineering Society. C) Supramolecular hydrogels with "host–guest" interactions. a) Schematic of a reversible ßCD/AD complex. b) Chemical structure of PEG4AD. c) In situ stiffening of hydrogel through incubating ßCD-containing hydrogel in PEG4AD solution. Hydrogel softening could be achieved by incubating the stiffened hydrogel in PBS or solution containing unmodified ßCD. C) Reproduced with permission.[161] Copyright 2016, The Royal Society of Chemistry.

from the SA1 and SA2 polymers, forming softer hydrogels. Furthermore, Shih and Lin reported a thiol-allylether hydrogel that was fabricated via a photo-click reaction of thiolated PVA, 4-arm PEG-allylether (PEG4AE) and mono-functional β-cyclodextrin-allylether (βCDAE). In situ stiffening/softening of the hydrogels was reversibly achieved by means of CD and adamantane (AD) supramolecular "host–guest" interactions (Figure 7C).[161] In the stiffening process, chemically immobilized "host" molecules (βCDAE) interacted with supplied 'guest' macromolecules (PEG4AD), leading to increased hydrogel crosslinking density and stiffness. If needed, such a stiffened hydrogel could be softened thermodynamically or through a competitive kinetic binding process. By incubating a stiffened hydrogel in solution containing soluble βCD, such unmodified βCD competed with immobilized βCD for binding to PEG4AD, resulting in a decrease in the hydrogel stiffness. Importantly, such a reversible change in hydrogel stiffness ranging from several hundreds to a few kilopascals was relevant to many cell fate processes.[18]

To achieve reversible mechanical stiffening or softening by using the second strategy, novel hydrogels in response to external stimuli (e.g., pH or temperature) have been developed recently. For example, a pH-responsive ABA triblock copolymer hydrogel with high biocompatibility was designed to reversibly adjust its stiffness, where A is poly(2-(diisopropylamino)ethyl methacrylate) (PDPA) and B is poly(2-(methacryloyloxy)ethyl phosphorylcholine) (PMPC) (**Figure 8**A).[162] At higher pH, the PDPA polymer chains became more deprotonated and thus obtained stronger interchain interactions, leading to a stiffer hydrogel. While at lower pH, the PDPA blocks were partially charged, and thus the hydrophobic interaction (or the physical crosslinking) became much weaker, resulting in a softer hydrogel. In addition, a thermoresponsive hybrid hydrogel capable of reversibly switching its stiffness was developed by Hackelbusch and co-workers (Figure 8B).[163] In their work, azide-functionalized of poly(*N*-(2-hydroxypropyl)-methacrylamide) (PHPMA) copolymers were first grafted with cyclooctyne-functionalized poly(*N*-isopropylacrylamide) (PNIPAAm) polymers. Then, PEG-bis(cyclooctyne) was used to crosslink these thermoresponsive comb polymers to form hydrogels via strain-promoted azide–alkyne cycloaddition (SPAAC)

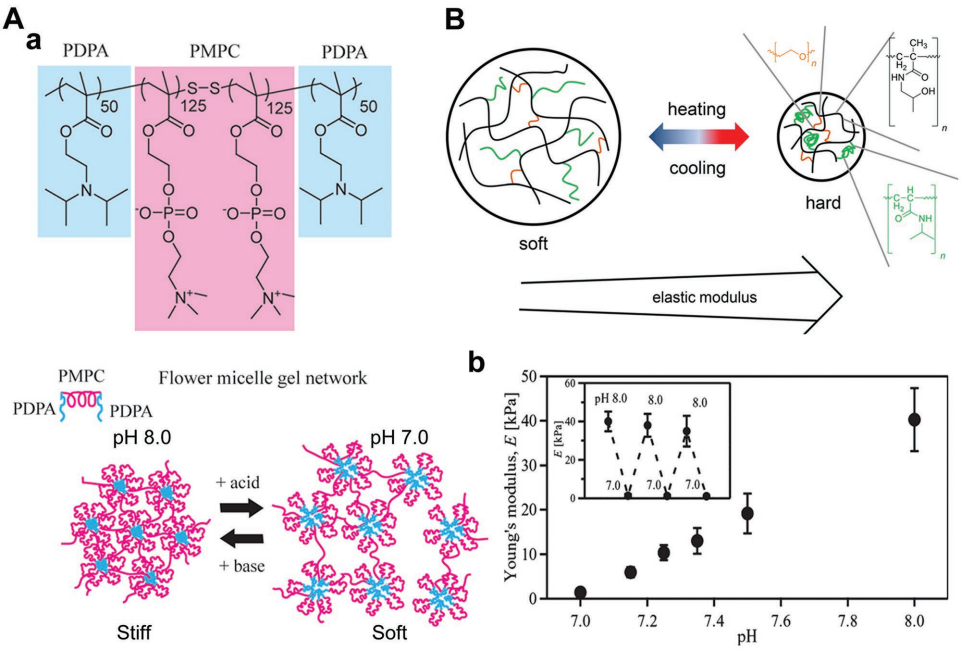

Figure 8. Engineering 3D mechanically reversible microenvironments in vitro using the second strategy. A) Mechanically reversible microenvironment engineered by pH-sensitive $PDPA_{50}$-$PMPC_{250}$-$PDPA_{50}$ triblock copolymer hydrogels. a) Schematic representation of the structural changes that occur within the hydrogel network on adjusting the pH by the addition of either acid or base. b) Young's modulus, *E*, determined for triblock copolymer hydrogels at various gel pH values. The inset illustrates the reversible modulation of *E* values over several pH cycles. A) Reproduced with permission.[162] Copyright 2011, ACS Publications. B) Mechanically reversible microenvironment engineered by thermo-responsive PNIPAAm-based hybrid hydrogels. Reproduced with permission.[163] Copyright 2015, Wiley-VCH.

reaction, which is regarded as a mild crosslinking method capable of encapsulating stem cells into hydrogels. With an increase in temperature, these PHPMA–PNIPAAm hydrogels could contract and expel water due to the formation of hydrophobic clusters composed of collapsed PNIPAAm side chains, leading to an increase in hydrogel stiffness. Hence, these thermoresponsive hydrogels reversibly expelled or took up water upon change of temperature, which resulted in a reversible change of elastic modulus. In a word, these 3D mechanically reversible microenvironments may act as versatile material platforms to further study stem cell mechanotransduction with great consistency.

4.2. Engineering 3D Spatiotemporal Stress/Strain Microenvironments of Stem Cells

In addition to ECM stiffness, mechanical stress and strain also play crucial roles in guiding stem cell fate, where the stress/strain applied to stem cells in 3D microenvironments mainly depends on their surrounding microenvironment (or the ECM). For instance, CPCs in heart, chondrocytes in cartilage and MSCs in bone marrow experience dynamic tensile stress, compression and shear stress, respectively, which accordingly guide their migration, proliferation and differentiation.[190–193] Hydrogels are often mechanically deformed (e.g., stretched or compressed) in vitro to reproduce the stress/strain microenvironment that stem cells experience in vivo. We herein review in the following sections on the effects of spatiotemporal stress/strain cues on stem cell fate.

4.2.1. Engineering Spatiotemporal Mechanical Stretching Microenvironments

Among various types of mechanical loading, stretching plays an important role in several physiological processes, including heart beating and muscle contraction. Hence, stretching has been utilized as a common mechanical cue to engineer stem cell microenvironments.[194] The simplest way to construct a controlled stress/strain microenvironment is to apply mechanical stretch to cell-laden hydrogels. For instance, CMPCs were encapsulated in 3D collagen/Matrigel hydrogels, which were then immobilized with two Velcro attachment points in tissue culture plates to achieve unidirectional constrained constructs.[194] The application of static unidirectional tensile strain was found to maintain CMPC viability, and especially enhance cardiac differentiation and induce cellular reorganization. Besides such a static stress/strain microenvironment, the dynamic stress/strain microenvironments based on 3D hydrogels have also been recently reported. For example, a microfabricated system that enabled dynamic stretching of arrayed cell-laden hydrogels was developed to study the relationship between dynamic mechanical cues and stem cell responses (**Figure 9**).[167] In this study, a off-stoichiometry thiol-ene-based polydimethylsiloxane (OSTE-PDMS) deformable membrane device was first fabricated. Then human MSCs/PEG-NB solutions were polymerized and bound to OSTE-PDMS membranes through a thiol-ene reaction (Figure 9A,B). Finally, the 3D cell-laden PEG-NB hydrogels could bulge up via a diaphragm pump and the top center of the hydrogels was increasingly displaced upwards with increasing pressure, suggesting that

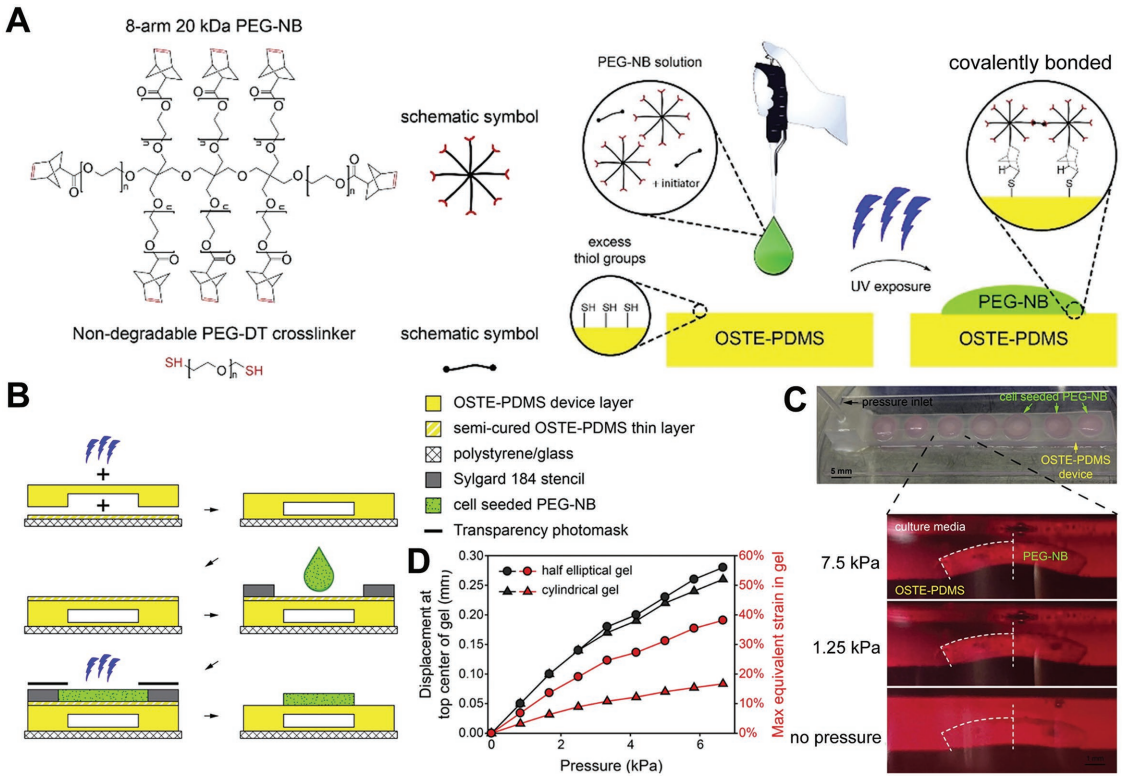

Figure 9. Engineering 3D dynamic mechanical stretching microenvironments in vitro. Hydrogel stretching via a deformable membrane platform. A) Demonstration of PEG-NB hydrogel bonding to OSTE-PDMS. B) Procedures to fabricate the OSTE-PDMS deformable membrane device and integrate and pattern cell-seeded PEG-NB hydrogels with the device. C) Example of the complete device with hMSCs seeded in the PEG-NB gel array and side view of a single PEG-NB hydrogel (outlined by white dashed line) in culture media deforming under increasing actuation pressure. D) Measured displacement of the hydrogel at its center and its corresponding maximum strain as a function of acturation pressure for two different hydrogel geometries. Reproduced with permission.[167] Copyright 2016, Elsevier.

the 3D cell-laden PEG-NB hydrogels were successfully stretched (Figure 9C,D). These cell-laden PEG-NB hydrogels bound to OSTE-PDMS membranes could be dynamically stretched when time-dependent actuation pressure was applied, and thus the encapsulated MSCs spread and differentiated into the contractile myofibroblast lineage. Additionally, gradient tensile strain microenvironments (e.g., linear, parabolic, and exponential gradients) were constructed by UV-triggered polymerization of GelMA in designed trapezoidal molds.[168] Although these systems were only used for 2D culture, they have great potentials to be extended for engineering 3D gradient strain microenvironments in vitro.

4.2.2. Engineering Spatiotemporal Compressive and/or Shear Stress Microenvironments

Compared with mechanical stretching, applying compressive or shear stress to the 3D hydrogels in a spatiotemporal manner is relatively convenient. Recently, a microfluidic chip-based approach combined with the GelMA hydrogels was used to create a range of gradient compressive strains in 3D microenvironments (**Figure 10**A).[169] A custom-designed microfluidic chip composed of treated glass and flexible PDMS membrane was fabricated first. Then, the outlet of the chip was plugged, and cells/GelMA suspensions were injected into the chip, resulting in convex PDMS deformation. The cell-laden GelMA hydrogels with gradient heights were formed after UV exposure through a concentric circular photomask. When unplugging the inlet and outlet, the convex PDMS membrane returned to the flat condition and thus applied gradient compressive forces on the hydrogels, resulting in gradient compressive strain microenvironments (from ≈65% to ≈15%). Additionally, Bian et al.[170] developed an agarose hydrogel-based dynamic compressive microenvironment with two loading modes, including unconfined axial compressive loading and sliding contact loading (Figure 10B). These dynamic compressive loadings were found to promote chondrogenesis in 3D hydrogels. Furthermore, Fisher and co-workers designed a tubular perfusion system (TPS) to apply both dynamic compressive and shear stress in a 3D microenvironment (Figure 10C).[171] Alginate hydrogel beads encapsulated with human MSCs were tightly packed in a tubular growth chamber. The medium was perfused using a pump through the growth chamber, passing stem cell-laden hydrogel beads and constantly exposing the encapsulated cells to shear stress. A designed roller was used to apply cyclic compressive stress onto tubular chambers. It was found that this dynamic mechanical microenvironment with combined mechanical stimulations might enhance chondrogenic differentiation in vitro.

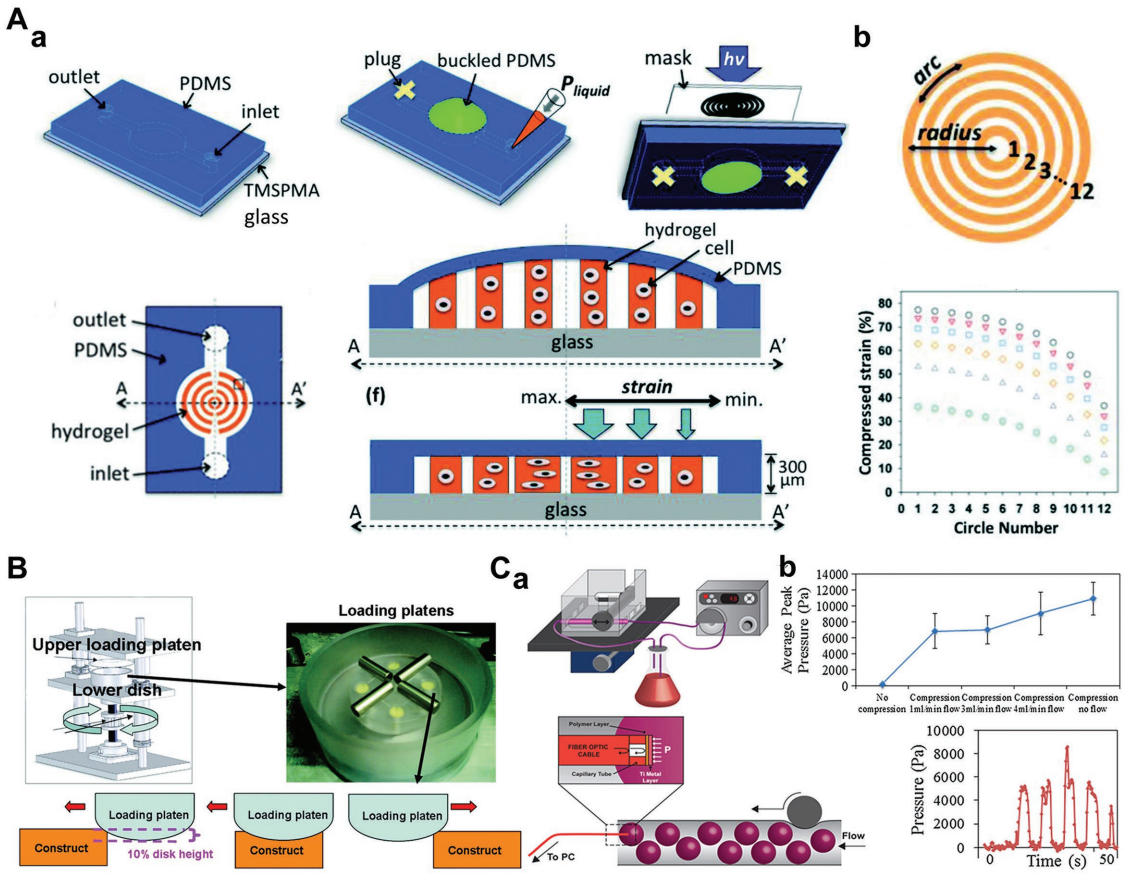

Figure 10. Engineering 3D compressive and/or shear stress microenvironments in vitro. A) Design of a microfluidic chip for a gradient compressive strain microenvironment. a) Schematic of the fabrication processes for gradient strain hydrogels in a microfluidic chip. b) The compressive strain percentages of the concentric hydrogel circles after releasing the liquid pressure. A) Reproduced with permission.[169] Copyright 2014, RSC Publishing. B) Design of a sliding contact bioreactor for a dynamic compressive microenvironment. The protocol produced 10% peak compressive loading coupled with oscillatory sliding contact, induced by curved loading platens sliding over the top surface of the constructs. B) Reproduced with permission.[170] Copyright 2010, Mary Ann Liebert, Inc. C) Design of a TPS bioreactor and its mechanical stimulations. a) Bioreactor assembly, the roller moves at a controlled speed provided by the rocker. The pressure detection unit with a close look of the detailed sensor design is also shown. b) Pressure measured inside the alginate beads. The upper figure shows the detected peak pressure at different conditions and the lower figure shows real time sensor response. C) Reproduced with permission.[171] Copyright 2015, Biomedical Engineering Society.

4.3. Engineering 3D Nonlinear Elastic Microenvironments of Stem Cells

Besides 3D stem cell microenvironments with linear mechanical properties as described above, the native ECM usually exhibits nonlinear elasticity, and stress stiffening is regarded as an important physiological mechanical behavior of ECM.[121] The onset of stiffening for ECM proteins often occurs at extremely low stress. In a recent work, Das et al.[9] developed a PIC-based hydrogel to study the effect of stress stiffening on human MSC fate in a 3D microenvironment, and these hydrogels demonstrated stress stiffening behaviors in a biologically relevant stress regime (≈0.1–30 Pa)[195] (**Figure 11**). Specifically, PICs (P1′–P6′) were copolymerized via a nickel (II)-catalyzed reaction, resulting in polymers with azide functionality. The catalyst to monomer molar ratio was varied to obtain P1′–P6′ with increasing molecular weight. Then, P1′–P6′ were reacted with BCN-GRGDS to synthesize cell-adhesive P1–P6 polymers with increasing polymer chain lengths (Figure 11A). Finally, P1–P6 hydrogels were fabricated by raising the temperature above ≈15 °C. The critical stress (σ_c) of P1–P6 hydrogels increased with increasing polymer length, from ≈9 Pa in the P1 gel to ≈19 Pa in the P6 gel (Figure 11B–D), while the stiffness and the adhesion ligand density were maintained the same. The human MSCs cultured in hydrogels with higher σ_c progressively favored osteogenic commitment over adipogenic lineage, which was mediated by the microtubule-associated protein DCAMKL1.

4.4. Engineering 3D Viscoelastic Microenvironments of Stem Cells

Most native tissues (e.g., adipose tissue,[196] brain,[197] and liver[198]) are viscoelastic and exhibit stress relaxation behaviors. However, most hydrogels for engineering 3D stem cell microenvironments are typically assumed to be elastic. To address this challenge, a well-defined P(NIPAAm-*r*-CA)-*b*-PEO-*b*-P(NIPAAm-*r*-CA) triblock copolymer (CA, coumarin

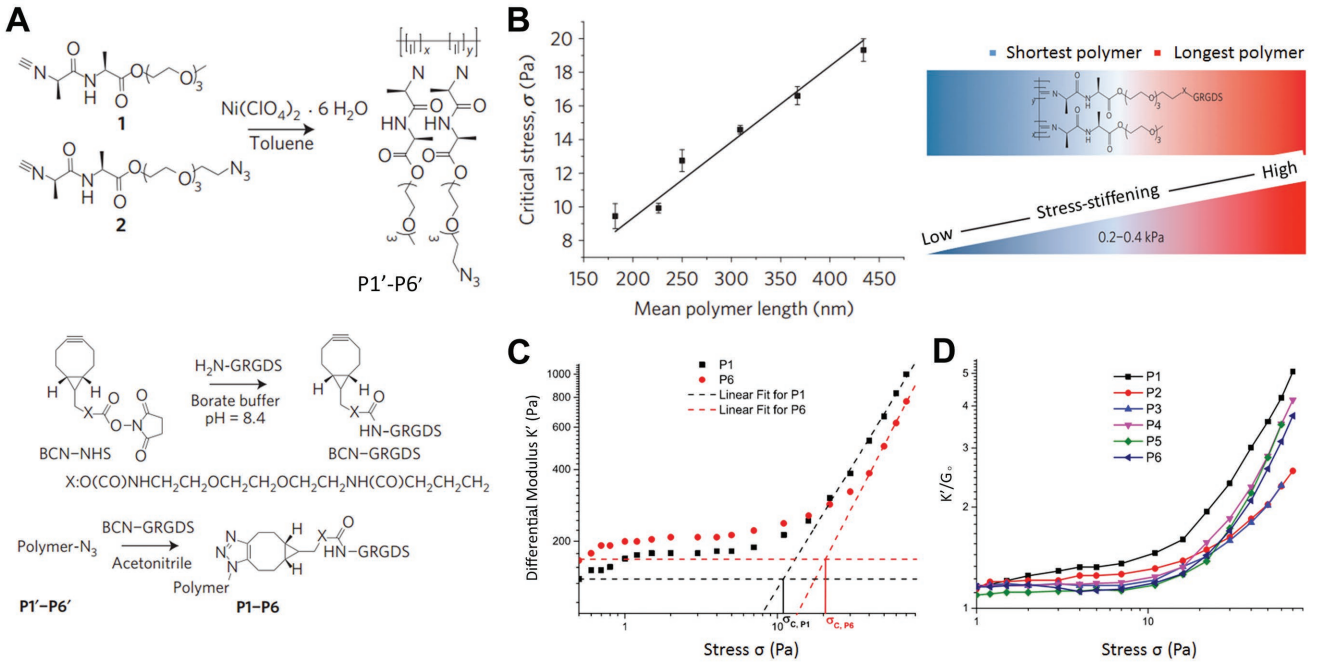

Figure 11. Engineering 3D nonlinear elastic microenvironments in vitro. A) Schematic of synthesis of GRGDS peptide functionalized polyisocyanopeptide with controlled stress stiffening. B) The critical stress increases linearly as a function of polymer length, and the schematic figure illustrates this overall trend. C) The nonlinear rheology data of polymer hydrogels P1–P6. The differential modulus K', scaled with storage modulus G_0, plotted as a function of applied stress σ. D) Overlay of the plots of differential modulus K' as a function of applied stress σ, for the gels of shortest (**P1**) and the longest (**P6**) polymer. σ_c denotes the critical stress for the onset of stress stiffening. Reproduced with permission.[9] Copyright 2015, Nature Publishing Group.

acrylate) was synthesized. When the polymer concentration was higher than the chain-overlap concentration, this triblock copolymer formed a physically crosslinked hydrogel upon heating, showing a stress relaxation behavior (**Figure 12**A).[172] Alternatively, a type of hydrazine-crosslinked PEG hydrogel with viscoelastic properties was also developed (Figure 12B).[173] Four-arm PEG macromers with aliphatic hydrazine end groups (4-H) were mixed with 4-arm PEG macromers with aliphatic aldehyde (4-AA), resulting in rapid formation of the hydrogel (4-H:4-AA) at physiological pH and temperature. Reversibly, covalent crosslinking could be weakened upon treatment with sodium cyanoborohydride, which reduced the hydrazone bond to the corresponding secondary hydrazine. The 4-H:4-AA hydrogel exhibited a frequency-dependent modulus, suggesting that it behaved as Maxwellian viscoelasticity. In these two examples, it was observed that both cell spreading and proliferation were enhanced in 3D viscoelastic microenvironments compared to that in 3D elastic microenvironments.

Furthermore, Chaudhuri et al.[10] developed an alginate hydrogel-based 3D microenvironment with controlled stress relaxation rate for studying murine MSC functions, independent of initial stiffness, adhesion-ligand density and degradation (Figure 12C). By decreasing the molecular weight of alginate, the stress relaxation rate of alginate hydrogels could be effectively increased due to altered chain mobility and connectivity in the polymer network. Furthermore, the alginate with low molecular weight could be covalently modified with short PEG spacers, which provided steric hindrance to alginate crosslinking and thus further enhanced stress relaxation of the alginate hydrogels. More importantly, initial elastic moduli showed no significant difference along with the altered stress relaxation rate, and they were stable during 7 d of culture. In these 3D viscoelastic microenvironments, cell spreading, proliferation, and differentiation (especially osteogenic differentiation) of MSCs were all enhanced when MSCs were cultured in hydrogels with higher stress relaxation rate. The authors explained that MSCs initially exerted forces on the 3D matrices, leading to resistance to such cell-generated forces in the matrices, which depended on the initial elastic moduli of the matrices. The viscoelastic matrices had an ability to gradually dissipate cell-generated forces due to mechanical yielding and remodeling of the matrices. Since the degree of such mechanical remodeling depended on the stress relaxation rate, the matrices with faster stress relaxation exhibited an increased clustering of embedded integrin motifs, which thus enhanced cell shape change, proliferation and osteogenic differentiation of MSCs.

5. Potential Biomedical Applications

The fate of stem cells can be directly regulated by tailoring their spatiotemporal mechanical microenvironments. Hence, modulation of stem cell behaviors (e.g., migration, proliferation, and differentiation) through spatiotemporal mechanical cues provides a unique strategy for biomedical applications, including stem-cell-based therapy, pathological study, tissue engineering, and organoid formation.

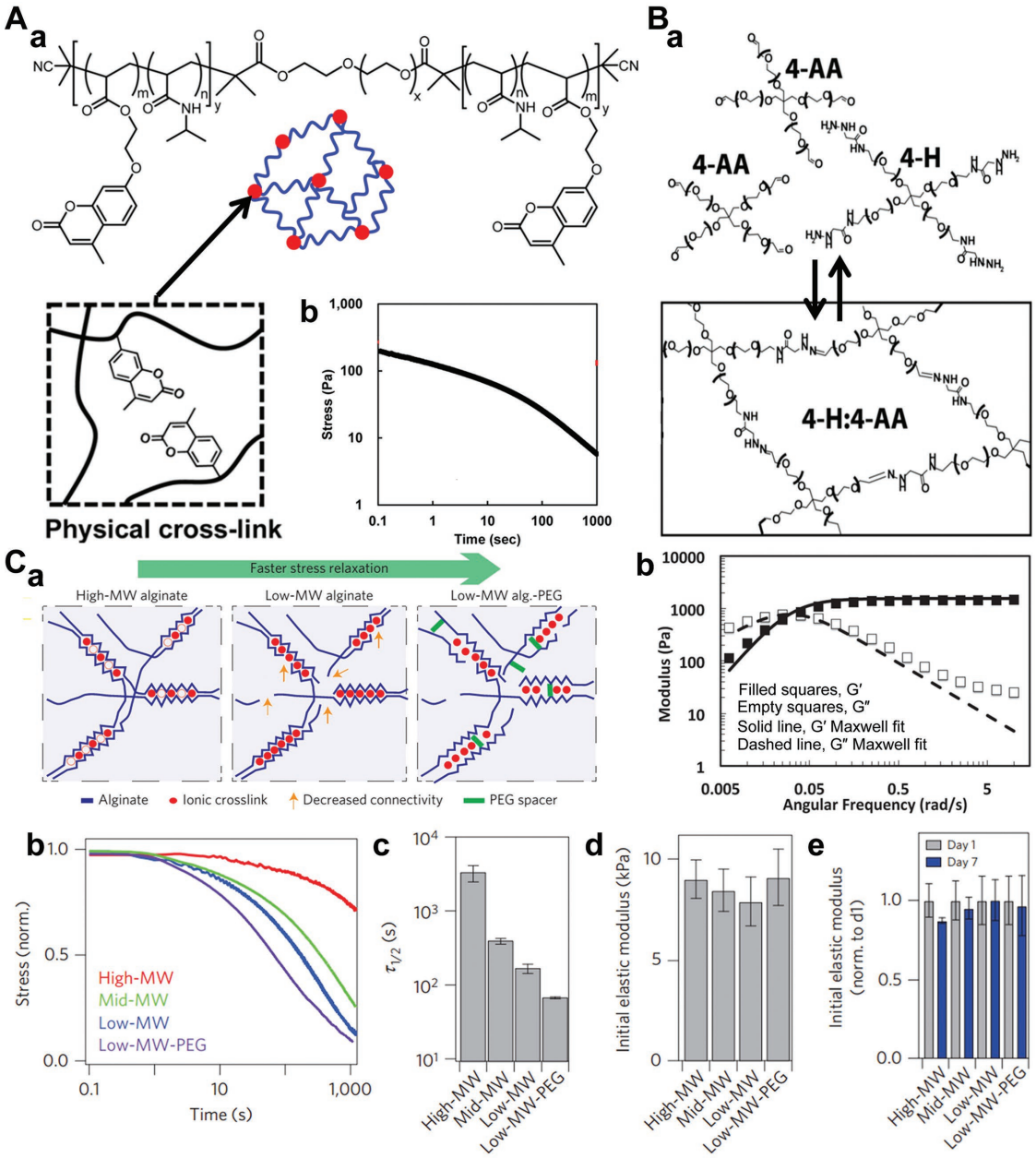

Figure 12. Engineering 3D viscoelastic microenvironments in vitro. A) ABA triblock copolymer hydrogel-based viscoelastic microenvironment. a) Chemical structure of the ABA triblock polymer and a conceptual illustration of ABA triblock copolymer hydrogel. b) Stress relaxation tests for the hydrogel at 37 °C. A) Reproduced with permission.[172] Copyright 2016, American Chemical Society. B) Hydrazone crosslinked PEG hydrogel-based viscoelastic microenvironment. a) Chemical structures of 4-H and 4-AA showing reversible gelation. b) 4-H:4-AA hydrogel shows a frequency-dependent modulus that is characteristic of a single-mode Maxwell viscoelastic fluid. B) Reproduced with permission.[173] Copyright 2013, Wiley-VCH. C) Alginate hydrogel-based viscoelastic microenvironment. a) Schematic depicting how to increase the rate of stress relaxation by lowering the molecular weight (MW) of alginate polymers and coupling of PEG spacers. b) Stress relaxation tests on hydrogels composed of alginates with different molecular weights, or low-MW alginate coupled to a PEG spacer (15% compressional strain). c) Quantification of timescale at which the stress is relaxed to half its original value, $\tau_{1/2}$, from stress relaxation tests in (b). d) Initial modulus measurements of hydrogels in (b). Differences between elastic moduli are not significant. e) Initial elastic modulus of alginate hydrogels after 1 d or 7 d in culture, normalized by the value at day 1. C) Reproduced with permission.[10] Copyright 2015, Nature Publishing Group.

5.1. Stem-Cell-Based Therapy

Stem-cell-based therapy is to treat a disease by using stem cells where the key is well controlled differentiation. Engineering appropriate mechanical microenvironments of stem cells is beneficial to achieve controlled cell differentiation for stem-cell-based therapy. For instance, Huebsch et al. developed an alginate-based void-forming hydrogel to transplant stem cells for bone regeneration (**Figure 13**A).[7] Alginate dialdehyde-based hydrolysable microspheres were encapsulated into bulk hydrogels, and

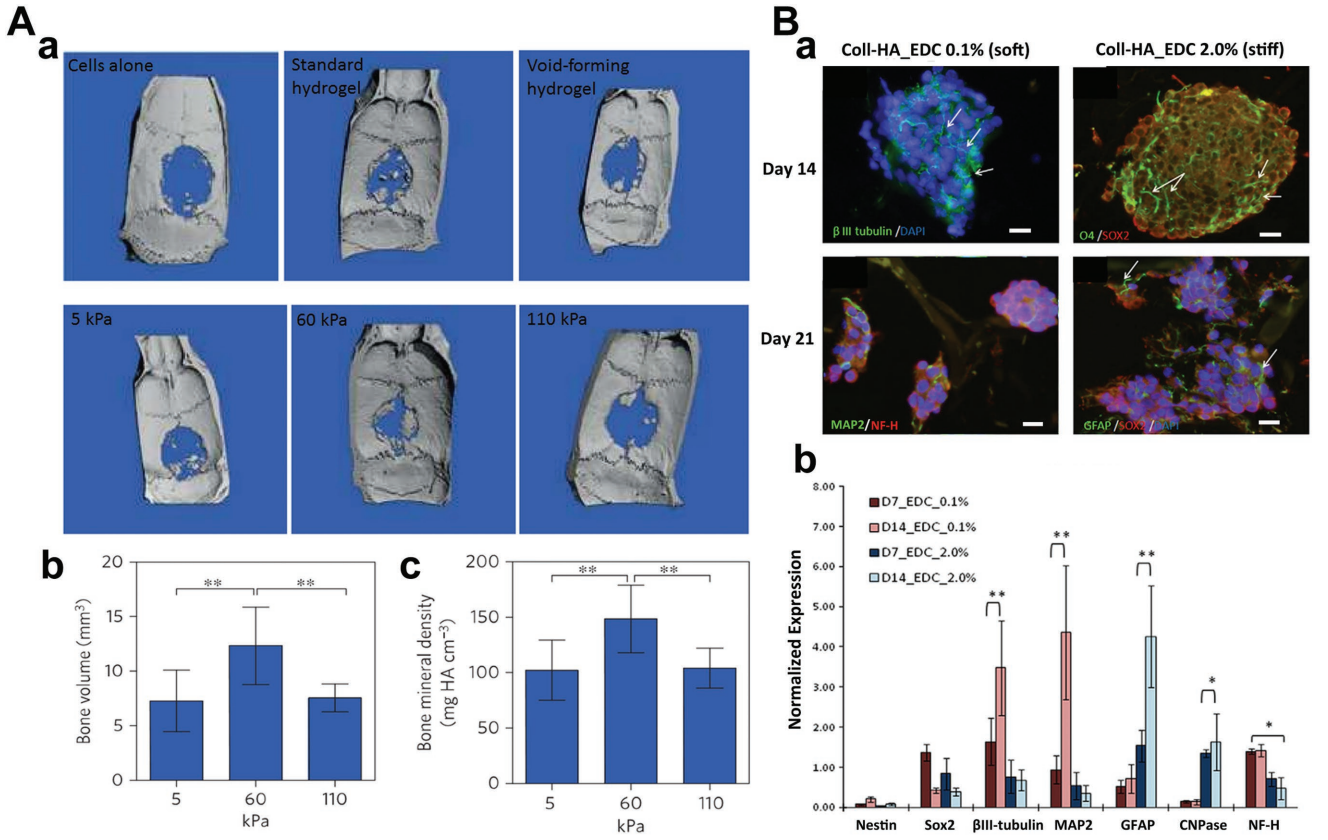

Figure 13. Engineering 3D spatiotemporal mechanical microenvironments for stem-cell-based therapy. A) Engineering of 3D mechanical softening microenvironment for transplanting hMSCs to bone tissue. a) Representative microcomputed tomographic (μCT) images of regeneration in nude rat cranial defects 12 weeks after inducing hMSCs in saline (cells alone), within standard hydrogels and within void-forming hydrogels. b) Representative μCT images of regeneration in nude rat cranial defects 12 weeks after hMSCs delivery in void-forming hydrogels of varying moduli. c,d) Quantitative analysis of total volume (c) and average bone mineral density (d) of regenerated bone. A) Reproduced with permission.[7] Copyright 2015, Nature Publishing Group. B) Engineering of 3D tunable mechanical microenvironment for delivering hMSCs into the spinal cord or brain. a) Immunohistochemistry of neuronal protein markers and glial protein markers for hMSCs in Col-HA_EDC 0.1% (1 kPa, soft) and Col-HA_EDC 2.0% (10 kPa, stiff). Scale bar: 200 μm. b) Quantitative real-time polymerase chain reaction results for neural lineage specific genes ($n = 3$, $^*P < 0.1$, $^{**}P < 0.05$). B) Reproduced with permission.[97] Copyright 2012, Elsevier.

hydrogel elasticity could be tuned by gradual generation of voids within the bulk hydrogels through regulation of microsphere degradation via hydrolysis. Human MSCs encapsulated in saline, hydrogels without degradable microspheres and the void-forming hydrogels were injected into 8-mm critical-sized cranial defects in nude mice. The transplanted human MSCs within the void-forming hydrogels exhibited increased formation of new bone, which indicated an obvious elasticity-dependent behavior. Bone volume and bone mineral density were significantly improved in the void-forming hydrogels with elastic modulus of 60 kPa compared to transplantation of human MSCs in other hydrogels (5 and 110 kPa). This indicated that the void-forming hydrogel with dynamically changed elasticity could be utilized as an efficient carrier for stem-cell-based bone regeneration. In another example, by controlling the stiffness of 3D collagen/hyaluronic acid matrices, human MSCs were directed toward neuronal differentiation in a soft matrix (≈1 kPa) but into a glial lineage in a relatively stiff matrix (≈10 kPa) (Figure 13B).[97] ß III-tubulin, MAP2, and NF-H are commonly expressed in neurons and regarded as the early, mid/late and late neuronal markers, respectively, while GFAP, CNPase, and O4 are recognized as typical glial protein markers (CNPase and O4 for oligodendrocytes and GFAP for astrocytes).[199–203] Both ß III-tubulin and MAP2 were significantly up-regulated after culture for 14 d in a soft matrix. Additionally, the expression of the NF-H gene increased dramatically after culture for 21 d, as confirmed by immunostaining, indicating that human MSCs probably needed more time to develop into mature neurons. In contrast, two glial protein markers (O4 and GFAP) were positively expressed, and the expression of GFAP and CNPase were upregulated after 14 d of culture in a stiff matrix, indicating successful differentiation of human MSCs into a glial lineage. These matrices with tunable stiffness had the ability to specifically manipulate human MSC fate toward neuronal or glial lineages and thus may be a useful platform for delivering human MSCs into the injured spinal cord or brain for stem cell therapy. Hence, by drawing together expertise in engineering and biology, it would be possible to improve these stem-cell-based therapies for future medical applications.

5.2. Pathological Study

Engineering 3D spatiotemporal mechanical microenvironments is an effective method to construct 3D disease models with

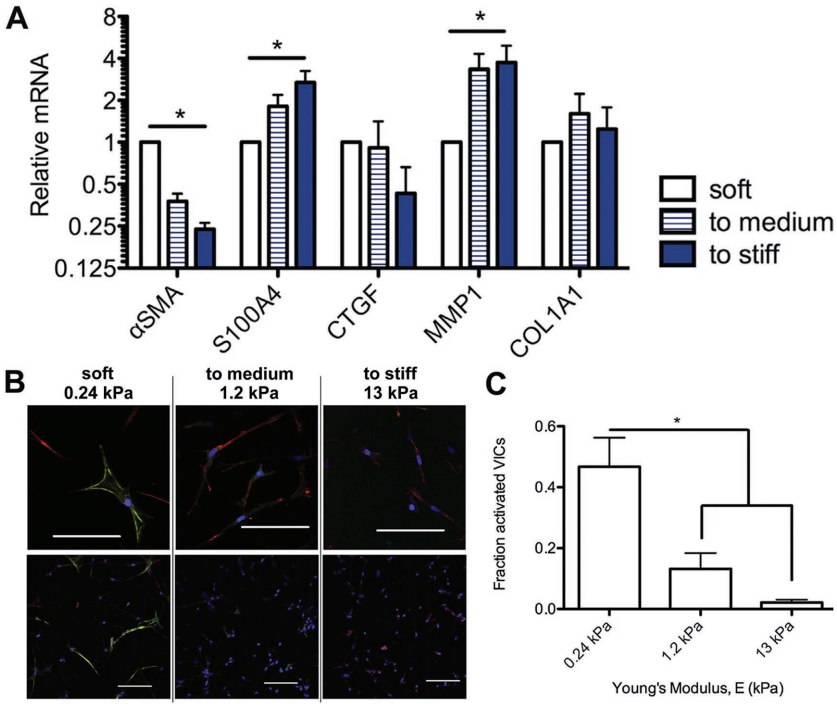

Figure 14. The 3D mechanical stiffening microenvironment mediates valvular interstitial cell phenotype decision to study fibroblast-to-myofibroblast transition associated with disease progression. A) qRT-PCR comparing genes of interest in soft (white), to medium (striped), and to stiff (solid) conditions. All genes were normalized to the L30 housekeeping gene. * indicates $p < 0.05$. B) Immunostaining for αSMA (green), f-actin (red) and nuclei (blue) in activated cells (myofibroblast phenotype) or deactivated cells (fibroblast phenotype). In soft gels, many cells exhibit aSMA stress fibers. In "to medium" gels, there are fewer cells positive for stress fibers, but diffuse aSMA is common. In "to stiff" gels, very little aSMA is present in either form. Scale bars: 100 µm. C) Fraction of activated valvular interstitial cells as defined by the presence of aSMA stress fibers was quantified. Activation decreased with increasing final modulus. Reproduced with permission.[33] Copyright 2015, Elsevier.

controlled disease conditions, which provides a great platform to study pathogenesis in vitro. For instance, dynamic stiffening of PEG-based hydrogels was used to manipulate VIC phenotype in a 3D mechanical microenvironment and investigate cell phenotypic changes involved in disease progression (**Figure 14**).[33] VICs were first encapsulated in 0.24 kPa MMP-degradable PEG hydrogels for 3 d to allow cell spreading. Then, after in situ stiffening of hydrogels to different moduli (1.2 or 13 kPa), the mRNA levels of myofibroblast markers, including alpha smooth muscle actin (αSMA) and CTGF, decreased with increasing stiffening of the hydrogels, while the fibroblast marker S100A4 showed an upward trend with an increase in stiffening. Overall, 42% of VICs exhibited organized stress fibers containing αSMA and exhibited the myofibroblast phenotype in a soft hydrogel (0.24 kPa). When the hydrogel-based microenvironment was stiffened to a modulus of 1.2 kPa, 13% of VICs expressed αSMA and still demonstrated the myofibroblast phenotype. In contrast, the cells cultured in a microenvironment stiffened to a modulus of 13 kPa exhibited significantly decreased αSMA (only 2.5% activation) and switched to a quiescent fibroblast phenotype. This in situ dynamic mechanical stiffening microenvironment may allow researchers to better understand VIC phenotypic changes, particularly the transition from fibroblasts to myofibroblasts, closely associated with human fibrotic diseases.

5.3. Tissue Engineering and Regenerative Medicine

Engineering 3D spatiotemporal mechanical microenvironments of stem cells also contributes to engineering of various tissues, since stem cells are the most promising cell source for tissue engineering. For instance, cyclic compressive loading and/or shear stress have been commonly used as dynamic mechanical cues to induce chondrogenic differentiation of MSCs, which have advanced our understanding of the role of dynamic compressive and/or shear stress microenvironments in cartilage tissue formation and has an aid to cartilage tissue engineering applications.[171,204] Recently, it has been reported that engineering a stiffness microenvironment (90 kPa) combined with appropriate biochemical composition can induce tenogenic/ligamentogenic differentiation of MSC and thus promote tenogenesis/ligamentogenesis.[205] Besides, the 3D dynamic tensile strain microenvironments fabricated via MMP-sensitive PEG-based hydrogels have also been confirmed to upregulate collagen III, tenascin C and decorin in MSCs and induce their tendon/ligament fibroblast phenotype.[206] Hence, these two kinds of engineered MSC mechanical microenvironments may contribute positively to tendon/ligament tissue engineering. Additionally, Murry's group studied the effects of cell microenvironment dimension (2D or 3D) and mechanical cues on differentiation and maturation of human cardiovascular progenitors (**Figure 15**A).[25] Cells derived from ESCs were encapsulated in collagen hydrogels and subjected to unstressed, static, and cyclic mechanical stress. Compared with 2D cultures, they found that a 3D microenvironment favored cardiac differentiation. Meanwhile, dynamic mechanical stress in 3D microenvironments improved the expression levels of cardiac markers, including cardiac troponin T (cTnT) and β-myosin heavy chain (βMHC), and enhanced active force production compared to no stress and static stress conditions. These results suggest the role of dynamic stress microenvironments in promoting cardiomyocyte structural and functional maturation. In addition, it indicates a potential strategy that could benefit our ability to predictably control the construction of organized and functional human cardiovascular tissues. Besides dynamic mechanical microenvironments in temporal control, nonuniform stiffness microenvironments in spatial control have also been widely studied in tissue engineering. Chatterjee et al. reported an osteoblast-encapsulated PEGDM hydrogel containing a broader stiffness gradient (≈10 to ≈300 kPa) to systematic screen osteoblast differentiation and mimic the 3D mechanical microenvironment of cells in vivo (Figure 15B).[157] It was indicated that the differentiation of osteoblasts could be influenced by mechanical properties of the hydrogels in

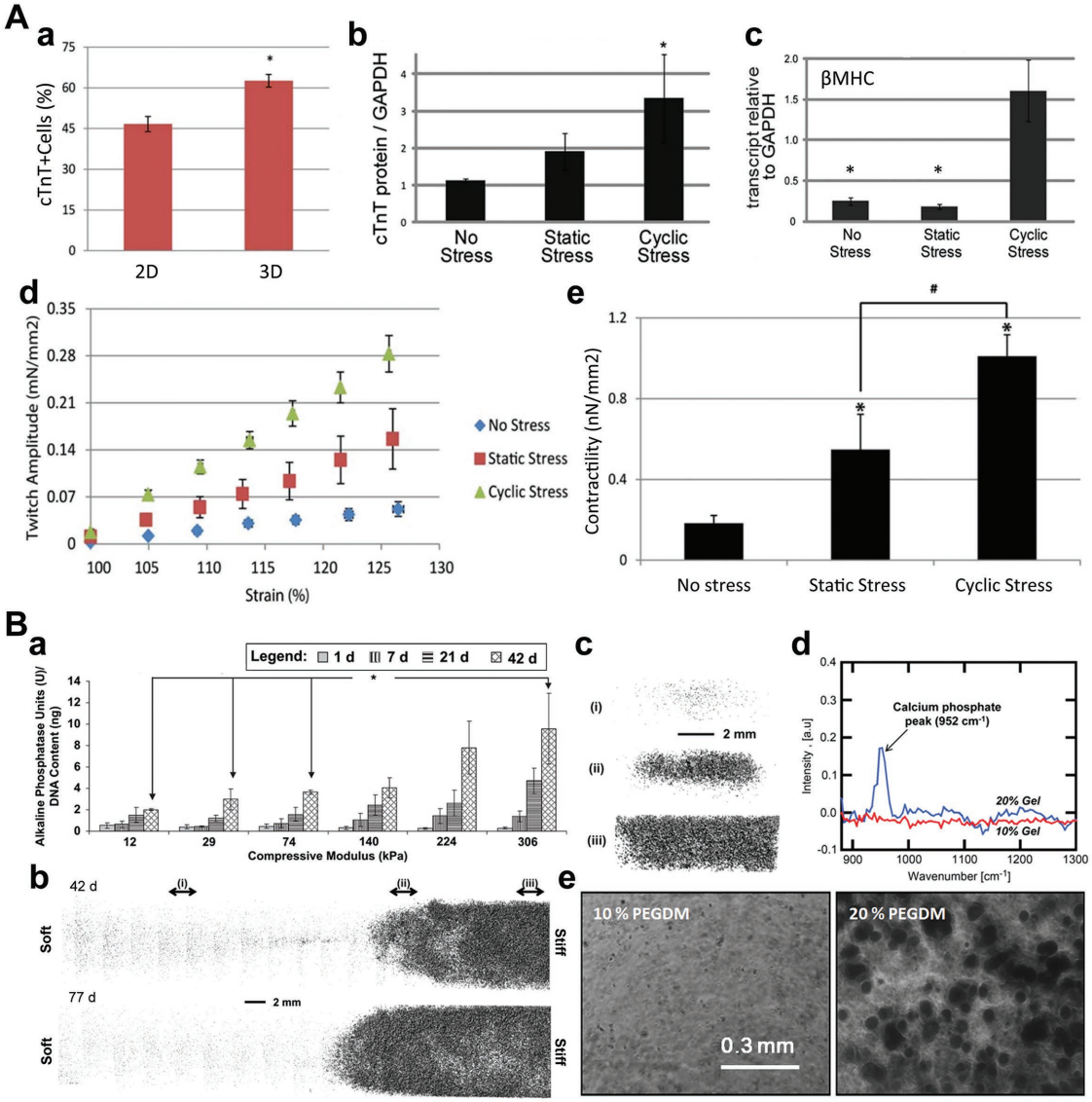

Figure 15. Engineering 3D spatiotemporal mechanical microenvironments for tissue engineering. A) 3D dynamic stress microenvironment for cardiovascular tissue engineering. a) Quantification of progenitor fate between 2D and 3D cultures. *, $p < 0.05$. b) Quantification of cTnT expression by Western blot. cTnT samples were normalized to GAPDH levels and given as fold over no stress conditioning. *, $p < 0.05$ with respect to no stress condition. c) Gene expression of βMHC analyzed by quantitative RT-PCR. *, $p < 0.05$ with respect to cyclic stress condition. d) Active force was increased with increasing strain of the engineered cardiovascular tissues. The slope of the active twitch amplitude and strain was defined as contractility as shown in (e). *, $p < 0.05$ with respect to no stress condition; #, $p < 0.05$. A) Reproduced with permission.[25] Copyright 2015, AlphaMed Press. B) 3D gradient stiffness microenvironment for generation of mineralized tissue gradient. a) Alkaline phosphatase expression activity (*, $p < 0.05$). b) Representative 3D reconstructions of the mineral deposits in the gradients at 42 d and 77 d from μCT scan of the hydrogel gradients. c) Images present cross-sectional view of the 42 d mineral distribution for 3 mm thick slices at three different positions [(i), (ii), (iii)] along the gradient as indicated in (b). d) Coherent anti-Stokes Raman scattering (CARS) imaging showing the composition of mineral deposits in hydrogels. e) Representative micrographs of cell-laden hydrogels stained with Alizarin Red S after 21 d of culture in growth medium. B) Reproduced with permission.[157] Copyright 2010, Elsevier.

the absence of biochemical cues. Furthermore, both alkaline phosphatase assay and μCT analysis demonstrated that osteogenic differentiation and subsequent mineralization were enhanced in PEGDM hydrogels with increased stiffness. Such cell differentiation-induced mineralization happened in the center of the hydrogels with lower stiffness and increased to the hydrogel edges with gradually increasing stiffness, finally forming gradient calcium phosphate deposits. Therefore, this spatially controlled stiffness microenvironment could induce graded osteogenesis and formation of a functional mineralized tissue gradient that could integrate hard and soft tissues such as ligament or tendon.

5.4. Organoid Formation

An organoid is a miniaturized and simplified version of an organ derived from various types of cells including stem cells,

which can self-organize in vitro in 3D and exhibit native-mimicking microanatomy. Organoid culture holds considerable potentials for investigating human development and disease, offering powerful new models for drug discovery and providing strategies for advancing precision and regenerative medicine.[207,208] Morphogenesis and organogenesis are closely related to mechanical cues. Different organs and even different tissue components within the same organ are characterized by distinct mechanical properties, and such mechanical modularity leads to the spatial differences that ultimately drive morphogenesis.[18,209] In addition, during organogenesis, mechanical cues along with other molecular cues are orchestrated in space and time to assemble multiple cell types into functional organs.[210] The complex and dynamic nature of this process has greatly hindered organoid culture in vitro. In particular, individual organs almost never develop in isolation, but rather concurrently with surrounding tissues and organs, which mechanically confine, impinge upon or pull on them continuously. These spatiotemporal mechanical cues that originate from surrounding tissues, which are notably absent in organoid culture, have been confirmed to affect the development of the optic cup, the intestine and the entire early mouse embryo.[211,212] Hence, engineering the spatiotemporal mechanical microenvironment to mimic the expansive growth of neighboring tissues and the consequent mechanical confinement to promote the formation of organoids will appear on the horizon.

6. Conclusions and Future Perspectives

In recent years, endeavors from multidisciplinary fields, including chemistry, physics, biology, and material science, have enabled extensive and intensive advances in the field of engineering 3D mechanical microenvironments of stem cells. Accumulating evidence suggests that stem cell fate is not only programmed by heredity, but also affected by the mechanical microenvironment in a spatiotemporal manner. Many studies have indicated that restoration of 3D mechanical microenvironments of stem cells in vitro holds great potentials to understand its role in guiding stem cell fate for stem-cell-based therapy, to generate functional tissues or organoids for tissue engineering and regenerative medicine, and to establish in vitro tissue models for physiological and pathological studies.

Recent advances in the design of hydrogel biomaterials with tunable physicochemical features and fabrication techniques (e.g., micropatterning,[213–215] bioprinting,[216–218] and microfluidics[219–221] etc.) have offered a versatile toolbox for engineering 3D spatiotemporal mechanical microenvironments of stem cells in vitro. Having reviewed the latest progress in such a fast developing field, we herein draw conclusions on the challenges and potential directions in the following three aspects for facilitating stem-cell-based studies toward biomedical applications in the future.

(1) Despite versatile modulation of the mechanical properties of hydrogels, they are still limited in providing in vivo-like spatiotemporal physical cues because of the complexity and heterogeneity of the native mechanical microenvironment of stem cells. Current functional hydrogel materials, including reversible hydrogels,[42] adaptable hydrogels,[222] and stimulus-responsive hydrogels[223] that can precisely capture extracellular matrix dynamics, may provide potential biomaterial candidates for better engineering of 3D spatiotemporal mechanical microenvironments in vitro. Besides, the development of both computational material science and computational biology may also make considerable contributions in engineering 3D mechanical microenvironments of stem cells, which is an emerging area. Taking full advantage of these computational tools, it may not only speed up the design of suitable biomaterials for engineering cell mechanical microenvironments, but also facilitate studies on how stem cells respond to these engineered cell mechanical microenvironments in vitro.[224,225]

(2) Until now, it remains a debate on the mechanisms how 3D spatiotemporal mechanical cues affect stem cell fate due to the crosstalk and interplay between signaling pathways and microenvironmental cues. To address this challenge, it is necessary to precisely characterize stem cell responses (e.g., cell size, shape, and volume etc.) to spatiotemporal mechanical cues. This first raises an unmet need to achieve in situ, real-time and even long-lasting and tracking of stem cells in 3D spatiotemporal mechanical microenvironments, which can benefit from the rocketing development of bioimaging and biosensing technologies.[226,227] Additionally, the detailed intracellular responses to 3D spatiotemporal mechanical microenvironments should also be considered, which relies on the combined studies at gene, molecular, and cellular levels to build intracellular and extracellular signaling communication networks that may promote to further understand the underlying mechanisms. Besides experimental strategies, mathematical modeling in a theoretical aspect can provides a powerful tool to predict stem cell behaviors. Moreover, such a computational strategy may conduct complicated investigations that cannot be achieved via experimental strategies. Hence, we believe that, with the progress in mathematical models for cell–microenvironment interactions in multiscale, theoretical, and mathematical models will offer more and more predictable and credible results in the near future.[228,229]

(3) A major motivation for engineering 3D mechanical microenvironments of stem cells is repair of injured tissues in vivo. Functional tissue constructs (e.g., the craniofacial bone substitute) for implantation purposes can be effectively fabricated by manipulating dental-derived MSC differentiation toward specific osteogenic lineages with the aid of in vitro 3D stem cell mechanical microenvironment engineering.[230] However, such in vitro-fabricated craniofacial bone substitutes may suffer limited regeneration capacity or even failure after transplantation because their own mechanical features may not match with that for native tissues or they may not afford the complicated mechanical microenvironments in vivo. Hence, in vivo engineering of 3D spatiotemporal mechanical microenvironments is greatly encouraged with the aim of in situ regeneration of functional tissue with improved performances. We believe that studies on in vivo engineering of 3D spatiotemporal mechanical microenvironments will be on the horizon with the rapid progress in stem cell biology, injectable biomaterials as well as corresponding injection techniques.[231,232]

Acknowledgements

Y.M. and M.L. contributed equally to this work. This work was financially supported by the National Natural Science Foundation of China (51502238, 11522219, 11602191), China Postdoctoral Science Foundation (2018M631172) and Opening Project of Key Laboratory of Shaanxi Province for Craniofacial Precision Medicine Research, College of Stomatology, Xi'an Jiaotong University (2016LHM-KFKT006). S.W. would like to acknowledge the support from the National Key Research and Development Program (2016YFC1101302).

Conflict of Interest

The authors declare no conflict of interest.

Keywords

cell microenvironments, hydrogels, mechanical cues, polymeric design, spatiotemporal control

Received: October 10, 2017
Revised: April 5, 2018
Published online:

[1] D. A. Robinton, G. Q. Daley, *Nature* **2012**, *481*, 295.
[2] P. Hou, Y. Li, X. Zhang, C. Liu, J. Guan, H. Li, T. Zhao, J. Ye, W. Yang, K. Liu, *Science* **2013**, *341*, 651.
[3] C. A. DeForest, D. A. Tirrell, *Nat. Mater.* **2015**, *14*, 523.
[4] F. M. Watt, W. T. Huck, *Nat. Rev. Mol. Cell Biol.* **2013**, *14*, 467.
[5] B. M. Baker, B. Trappmann, W. Y. Wang, M. S. Sakar, I. L. Kim, V. B. Shenoy, J. A. Burdick, C. S. Chen, *Nat. Mater.* **2015**, *14*, 1262.
[6] X. Yao, R. Peng, J. D. Ding, *Adv. Mater.* **2013**, *25*, 5257.
[7] N. Huebsch, E. Lippens, K. Lee, M. Mehta, S. T. Koshy, M. C. Darnell, R. M. Desai, C. M. Madl, M. Xu, X. Zhao, *Nat. Mater.* **2015**, *14*, 1269.
[8] A. D. Doyle, N. Carvajal, A. Jin, K. Matsumoto, K. M. Yamada, *Nat. Commun.* **2015**, *6*, 8720.
[9] R. K. Das, V. Gocheva, R. Hammink, O. F. Zouani, A. E. Rowan, *Nat. Mater.* **2016**, *15*, 318.
[10] O. Chaudhuri, L. Gu, D. Klumpers, M. Darnell, S. A. Bencherif, J. C. Weaver, N. Huebsch, H. P. Lee, E. Lippens, G. N. Duda, D. J. Mooney, *Nat. Mater.* **2016**, *15*, 326.
[11] P. Lu, K. Takai, V. M. Weaver, Z. Werb, *Cold Spring Harbor Perspect. Biol.* **2011**, *3*, a005058.
[12] C. Bonnans, J. Chou, Z. Werb, *Nat. Rev. Mol. Cell Biol.* **2014**, *15*, 786.
[13] F. Gattazzo, A. Urciuolo, P. Bonaldo, *Biochim. Biophys. Acta, Gen. Subj.* **2014**, *1840*, 2506.
[14] R. Sunyer, V. Conte, J. Escribano, A. Elosegui-Artola, A. Labernadie, L. Valon, D. Navajas, J. M. García-Aznar, J. J. Muñoz, P. Roca-Cusachs, *Science* **2016**, *353*, 1157.
[15] J. D. Humphrey, E. R. Dufresne, M. A. Schwartz, *Nat. Rev. Mol. Cell Biol.* **2014**, *15*, 802.
[16] J. H. Wen, L. G. Vincent, A. Fuhrmann, Y. S. Choi, K. C. Hribar, H. Taylor-Weiner, S. Chen, A. J. Engler, *Nat. Mater.* **2014**, *13*, 979.
[17] B. Trappmann, C. S. Chen, *Curr. Opin. Biotechnol.* **2013**, *24*, 948.
[18] A. J. Engler, S. Sen, H. L. Sweeney, D. E. Discher, *Cell* **2006**, *126*, 677.
[19] E. Santos, R. M. Hernández, J. L. Pedraz, G. Orive, *Trends Biotechnol.* **2012**, *30*, 331.
[20] R. J. Pelham, Y.-l. Wang, *Proc. Natl. Acad. Sci. USA* **1997**, *94*, 13661.
[21] G. Jiang, A. H. Huang, Y. Cai, M. Tanase, M. P. Sheetz, *Biophys. J.* **2006**, *90*, 1804.
[22] R. McBeath, D. M. Pirone, C. M. Nelson, K. Bhadriraju, C. S. Chen, *Dev. Cell* **2004**, *6*, 483.
[23] N. Huebsch, P. R. Arany, A. S. Mao, D. Shvartsman, O. A. Ali, S. A. Bencherif, J. Rivera-Feliciano, D. J. Mooney, *Nat. Mater.* **2010**, *9*, 518.
[24] E. Cukierman, R. Pankov, D. R. Stevens, K. M. Yamada, *Science* **2001**, *294*, 1708.
[25] J. L. Ruan, N. L. Tulloch, M. Saiget, S. L. Paige, M. V. Razumova, M. Regnier, K. C. Tung, G. Keller, L. Pabon, H. Reinecke, C. E. Murry, *Stem Cells* **2015**, *33*, 2148.
[26] H. Geckil, F. Xu, X. Zhang, S. Moon, U. Demirci, *Nanomedicine* **2010**, *5*, 469.
[27] I. Hopp, A. Michelmore, L. E. Smith, D. Robinson, A. Bachhuka, A. Mierczynska, K. Vasilev, *Biomaterials* **2013**, *34*, 5070.
[28] R. T. Justin, A. J. Engler, *PLoS One* **2011**, *6*, e15978.
[29] A. M. Kloxin, J. A. Benton, K. S. Anseth, *Biomaterials* **2010**, *31*, 1.
[30] P. Wang, W. Tsai, N. H. Voelcker, *Acta Biomater.* **2012**, *8*, 519.
[31] S. H. Oh, D. B. An, T. H. Kim, J. H. Lee, *Acta Biomater.* **2016**, *35*, 23.
[32] S. Khetan, M. Guvendiren, W. R. Legant, D. M. Cohen, C. S. Chen, J. A. Burdick, *Nat. Mater.* **2013**, *12*, 458.
[33] K. M. Mabry, R. L. Lawrence, K. S. Anseth, *Biomaterials* **2015**, *49*, 47.
[34] M. Guvendiren, J. A. Burdick, *Nat. Commun.* **2012**, *3*, 792.
[35] L. B. Hazeltine, J. A. Selekman, S. P. Palecek, *Biotechnol. Adv.* **2013**, *31*, 1002.
[36] J. Jiang, E. T. Papoutsakis, *Adv. Healthcare Mater.* **2013**, *2*, 25.
[37] M. Guvendiren, J. A. Burdick, *Curr. Opin. Biotechnol.* **2013**, *24*, 841.
[38] A. Higuchi, Q. D. Ling, Y. Chang, S.-T. Hsu, A. Umezawa, *Chem. Rev.* **2013**, *113*, 3297.
[39] Y. Sun, C. S. Chen, J. Fu, *Annu. Rev. Biophys.* **2012**, *41*, 519.
[40] F. Guilak, D. M. Cohen, B. T. Estes, J. M. Gimble, W. Liedtke, C. S. Chen, *Cell Stem Cell* **2009**, *5*, 17.
[41] K. Uto, J. H. Tsui, C. A. DeForest, D. H. Kim, *Prog. Polym. Sci.* **2017**, *65*, 53.
[42] A. M. Rosales, K. S. Anseth, *Nat. Rev. Mater.* **2016**, *1*, 15012.
[43] J. Kim, R. C. Hayward, *Trends Biotechnol.* **2012**, *30*, 426.
[44] W. P. Daley, S. B. Peters, M. Larsen, *J. Cell Sci.* **2008**, *121*, 255.
[45] M. M. Nava, M. T. Raimondi, R. Pietrabissa, *J. Biomed. Biotechnol.* **2012**, *2012*, 797410.
[46] J. Heino, J. Kapyla, *Curr. Pharm. Des.* **2009**, *15*, 1309.
[47] H. E. Balcioglu, H. van Hoorn, D. M. Donato, T. Schmidt, E. H. J. Danen, *J. Cell Sci.* **2015**, *128*, 1316.
[48] N. Wang, J. D. Tytell, D. E. Ingber, *Nat. Rev. Mol. Cell Biol.* **2009**, *10*, 75.
[49] B. Geiger, J. P. Spatz, A. D. Bershadsky, *Nat. Rev. Mol. Cell Biol.* **2009**, *10*, 21.
[50] G. Maya-Espinosa, O. Collazo-Navarrete, D. Millan-Aldaco, M. Palomero-Rivero, G. Guerrero-Flores, R. Drucker-Colin, L. Covarrubias, M. Guerra-Crespo, *Stem Cells* **2015**, *33*, 491.
[51] Y. W. Yan, L. M. Martin, D. B. Bosco, J. L. Bundy, R. S. Nowakowski, Q. X. A. Sang, Y. Li, *Biomaterials* **2015**, *73*, 231.
[52] E. L. Papadopoulou, A. Samara, M. Barberoglou, A. Manousaki, S. N. Pagakis, E. Anastasiadou, C. Fotakis, E. Stratakis, *Tissue Eng., Part C* **2010**, *16*, 497.
[53] D. Sasaki, T. Shimizu, S. Masuda, J. Kobayashi, K. Itoga, Y. Tsuda, J. K. Yamashita, M. Yamato, T. Okano, *Biomaterials* **2009**, *30*, 4384.
[54] L. Adamo, O. Naveiras, P. L. Wenzel, S. Mckinneyfreeman, P. Mack, J. Graciasancho, A. Suchydicey, M. Yoshimoto, M. W. Lensch, M. C. Yoder, *Nature* **2009**, *459*, 1131.
[55] N. F. Huang, B. Patlolla, O. J. Abilez, H. Sharma, J. Rajadas, R. E. Beygui, C. K. Zarins, J. P. Cooke, *Acta Biomater.* **2010**, *6*, 4614.
[56] Y. Jiang, B. N. Jahagirdar, R. L. Reinhardt, R. E. Schwartz, C. D. Keene, X. R. Ortiz-Gonzalez, M. Reyes, T. Lenvik, T. Lund, M. Blackstad, *Nature* **2002**, *418*, 41.

[57] I. L. Ivanovska, J.-W. Shin, J. Swift, D. E. Discher, *Trends Cell Biol.* **2015**, *25*, 523.
[58] E. Ozcivici, Y. K. Luu, B. Adler, Y. Qin, J. Rubin, S. Judex, C. T. Rubin, *Nat. Rev. Rheumatol.* **2010**, *6*, 50.
[59] U. A. Gurkan, O. Akkus, *Ann. Biomed. Eng.* **2008**, *36*, 1978.
[60] X. Gao, X. Zhang, H. Tong, B. Lin, J. Qin, *Electrophoresis* **2011**, *32*, 3431.
[61] Y. Morita, S. Watanabe, Y. Ju, B. Xu, *Acta Bioeng. Biomech.* **2013**, *15*, 71.
[62] C. C. Huang, K. L. Hagar, L. E. Frost, Y. Sun, H. S. Cheung, *Stem Cells* **2004**, *22*, 313.
[63] S. D. Thorpe, C. T. Buckley, T. Vinardell, F. J. O. Brien, V. A. Campbell, D. J. Kelly, *Biochem. Biophys. Res. Commun.* **2008**, *377*, 458.
[64] V. Bassaneze, V. G. Barauna, C. Laviniramos, J. Kalil, I. T. Schettert, A. A. Miyakawa, J. E. Krieger, *Stem Cells Dev.* **2010**, *19*, 371.
[65] J. R. Glossop, S. H. Cartmell, *Gene Expression Patterns* **2009**, *9*, 381.
[66] S. Ghazanfari, M. Tafazzolishadpour, M. A. Shokrgozar, *Biochem. Biophys. Res. Commun.* **2009**, *388*, 601.
[67] Z. Gong, L. E. Niklason, *FASEB J.* **2008**, *22*, 1635.
[68] J. A. Panadero, S. Lanceros-Mendez, J. L. G. Ribelles, *Acta Biomater.* **2016**, *33*, 1.
[69] X. Gao, X. Zhang, H. Xu, B. Zhou, W. Wen, J. Qin, *Biomicrofluidics* **2014**, *8*, 52008.
[70] S. Rafii, D. Lyden, *Nat. Med.* **2003**, *9*, 702.
[71] A. D. Durbin, A. I. Gotlieb, *Cardiovasc. Pathol.* **2002**, *11*, 69.
[72] N. M. Rajamannan, F. J. Evans, E. Aikawa, K. J. Grande-Allen, L. L. Demer, D. D. Heistad, C. A. Simmons, K. S. Masters, P. Mathieu, K. D. O'Brien, F. J. Schoen, D. A. Towler, A. P. Yoganathan, C. M. Otto, *Circulation* **2011**, *124*, 1783.
[73] A. C. Liu, V. R. Joag, A. I. Gotlieb, *Am. J. Pathol.* **2007**, *171*, 1407.
[74] J. H. C. Wang, Q. P. Guo, B. Li, *J. Hand Ther.* **2012**, *25*, 133.
[75] J. L. Cook, C. Purdam, *Br. J. Sports Med.* **2012**, *46*, 163.
[76] J. H. C. Wang, *J. Biomech.* **2006**, *39*, 1563.
[77] J. Y. Zhang, J. H. C. Wang, *Bmc Musculoskeletal Disord.* **2010**, *11*, 10.
[78] J. Y. Zhang, T. Pan, Y. Liu, J. H. C. Wang, *J. Orthop. Res.* **2010**, *28*, 1178.
[79] T. A. L. Wren, S. A. Yerby, G. S. Beaupre, D. R. Carter, *Clin. Biomech.* **2001**, *16*, 245.
[80] L. G. Vincent, Y. S. Choi, B. Alonso-Latorre, J. C. del Álamo, A. J. Engler, *Biotech. J.* **2013**, *8*, 472.
[81] Y. Katayama, M. Battista, W. M. Kao, A. Hidalgo, A. J. Peired, S. A. Thomas, P. S. Frenette, *Cell* **2006**, *124*, 407.
[82] A. S. Rowlands, P. A. George, J. J. Cooper-White, *Am. J. Physiol.: Cell Physiol.* **2008**, *295*, C1037.
[83] C. M. Lo, H. B. Wang, M. Dembo, Y. l. Wang, *Biophys. J.* **2000**, *79*, 144.
[84] F. Liu, J. D. Mih, B. S. Shea, A. T. Kho, A. S. Sharif, A. M. Tager, D. J. Tschumperlin, *J. Cell Biol.* **2010**, *190*, 693.
[85] K. W. Yong, Y. Li, G. Huang, T. J. Lu, W. K. Z. W. Safwani, B. Pingguan-Murphy, F. Xu, *Am. J. Physiol.: Heart Circ. Physiol.* **2015**, *309*, H532.
[86] A. K. Schroer, W. D. Merryman, *J. Cell Sci.* **2015**, *128*, 1865.
[87] O. A. Lozoya, E. Wauthier, R. A. Turner, C. Barbier, G. D. Prestwich, F. Guilak, R. Superfine, S. R. Lubkin, L. M. Reid, *Biomaterials* **2011**, *32*, 7389.
[88] B. M. Gillette, J. A. Jensen, M. Wang, J. Tchao, S. K. Sia, *Adv. Mater.* **2010**, *22*, 686.
[89] S. Kang, J. B. Park, T. J. Lee, S. Ryu, S. H. Bhang, W. G. La, M. K. Noh, B. H. Hong, B.-S. Kim, *Carbon* **2015**, *83*, 162.
[90] W. S. Toh, T. C. Lim, M. Kurisawa, M. Spector, *Biomaterials* **2012**, *33*, 3835.
[91] S. J. Bryant, R. J. Bender, K. L. Durand, K. S. Anseth, *Biotechnol. Bioeng.* **2004**, *86*, 747.
[92] R. A. Marklein, D. E. Soranno, J. A. Burdick, *Soft Matter* **2012**, *8*, 8113.
[93] E. Dawson, G. Mapili, K. Erickson, S. Taqvi, K. Roy, *Adv. Drug Delivery Rev.* **2008**, *60*, 215.
[94] N. S. Hwang, S. Varghese, J. Elisseeff, *Adv. Drug Delivery Rev.* **2008**, *60*, 199.
[95] K. W. Yong, Y. Li, F. Liu, B. Gao, T. J. Lu, W. A. B. W. Abas, W. K. Z. W. Safwani, B. Pingguan-Murphy, Y. Ma, F. Xu, *Sci. Rep.* **2016**, *6*, 33067.
[96] E. M. Chandler, C. M. Berglund, J. S. Lee, W. J. Polacheck, J. P. Gleghorn, B. J. Kirby, C. Fischbach, *Biotechnol. Bioeng.* **2011**, *108*, 1683.
[97] G. J. Her, H. C. Wu, M. H. Chen, M. Y. Chen, S. C. Chang, T. W. Wang, *Acta Biomater.* **2013**, *9*, 5170.
[98] K. Xu, K. Narayanan, F. Lee, K. H. Bae, S. Gao, M. Kurisawa, *Acta Biomater.* **2015**, *24*, 159.
[99] T. C. Lim, W. S. Toh, L. S. Wang, M. Kurisawa, M. Spector, *Biomaterials* **2012**, *33*, 3446.
[100] X. Li, S. Chen, J. Li, X. Wang, J. Zhang, N. Kawazoe, G. Chen, *Polymers* **2016**, *8*, 269.
[101] W. Schuurman, P. A. Levett, M. W. Pot, P. R. van Weeren, W. J. Dhert, D. W. Hutmacher, F. P. Melchels, T. J. Klein, J. Malda, *Macromol. Biosci.* **2013**, *13*, 551.
[102] C. Chung, B. L. Pruitt, S. C. Heilshorn, *Biomater. Sci.* **2013**, *1*, 1082.
[103] W. T. Hsieh, Y. S. Liu, Y. H. Lee, M. G. Rimando, K. H. Lin, O. K. Lee, *Acta Biomater.* **2016**, *32*, 210.
[104] L. S. Wang, J. E. Chung, P. P. Y. Chan, M. Kurisawa, *Biomaterials* **2010**, *31*, 1148.
[105] Z. Li, X. Guo, S. Matsushita, J. Guan, *Biomaterials* **2011**, *32*, 3220.
[106] S. Q. Liu, Q. Tian, J. L. Hedrick, J. H. P. Hui, P. L. R. Ee, Y. Y. Yang, *Biomaterials* **2010**, *31*, 7298.
[107] Y. S. Pek, A. C. Wan, J. Y. Ying, *Biomaterials* **2010**, *31*, 385.
[108] L. S. Wang, C. Du, J. E. Chung, M. Kurisawa, *Acta Biomater.* **2012**, *8*, 1826.
[109] M. Nii, J. H. Lai, M. Keeney, L. H. Han, A. Behn, G. Imanbayev, F. Yang, *Acta Biomater.* **2013**, *9*, 5475.
[110] L. S. Wang, C. Du, W. S. Toh, A. C. Wan, S. J. Gao, M. Kurisawa, *Biomaterials* **2014**, *35*, 2207.
[111] B. Duan, L. A. Hockaday, E. Kapetanovic, K. H. Kang, J. T. Butcher, *Acta Biomater.* **2013**, *9*, 7640.
[112] J. L. Young, A. J. Engler, *Biomaterials* **2011**, *32*, 1002.
[113] S. Khetan, J. S. Katz, J. A. Burdick, *Soft Matter* **2009**, *5*, 1601.
[114] Y. Ma, Y. Ji, G. Huang, K. Ling, X. Zhang, F. Xu, *Biofabrication* **2015**, *7*, 044105.
[115] L. Macri-Pellizzeri, B. Pelacho, A. Sancho, O. Iglesias-Garcia, A. M. Simon-Yarza, M. Soriano-Navarro, S. Gonzalez-Granero, J. M. Garcia-Verdugo, E. M. De-Juan-Pardo, F. Prosper, *Tissue Eng., Part A* **2015**, *21*, 1633.
[116] S. Choi, J. Kim, *J. Mater. Chem. B* **2015**, *3*, 1479.
[117] Y. Aizawa, S. C. Owen, M. S. Shoichet, *Prog. Polym. Sci.* **2012**, *37*, 645.
[118] M. W. Tibbitt, K. S. Anseth, *Biotechnol. Bioeng.* **2009**, *103*, 655.
[119] M. Lutolf, J. Hubbell, *Nat. Biotechnol.* **2005**, *23*, 47.
[120] D. Seliktar, *Science* **2012**, *336*, 1124.
[121] C. Storm, J. J. Pastore, F. C. MacKintosh, T. C. Lubensky, P. A. Janmey, *Nature* **2005**, *435*, 191.
[122] Q. Wen, P. A. Janmey, *Exp. Cell Res.* **2013**, *319*, 2481.
[123] J. P. Winer, S. Oake, P. A. Janmey, *PLoS One* **2009**, *4*, e6382.
[124] R. J. Petrie, N. Gavara, R. S. Chadwick, K. M. Yamada, *J. Cell Biol.* **2012**, *197*, 439.
[125] B. H. Ji, B. Huo, *Acta Mech. Sin.* **2013**, *29*, 469.
[126] R. J. Petrie, K. M. Yamada, *J. Cell Sci.* **2012**, *125*, 5917.
[127] C. Müller, A. Müller, T. Pompe, *Soft Matter* **2013**, *9*, 6207.
[128] J. Chen, K. Wright, M. Birch, *Acta Mech. Sin.* **2014**, *30*, 2.
[129] Y. D. Park, N. Tirelli, J. A. Hubbell, *Biomaterials* **2003**, *24*, 893.

[130] C. T. W. P. Foo, J. S. Lee, W. Mulyasasmita, A. Parisi-Amon, S. C. Heilshorn, *Proc. Natl. Acad. Sci. USA* **2009**, *106*, 22067.
[131] X. Zhao, N. Huebsch, D. J. Mooney, Z. Suo, *J. Appl. Phys.* **2010**, *107*, 063509.
[132] J. Zidek, A. Milchev, J. Jancar, T. A. Vilgis, in *Intelligent Hydrogels*, Progress in Colloid and Polymer Science, Vol. *140*, (Eds: G. Sadowski, W. Richtering), Springer, Cham, Switzerland **2013**, p. 223.
[133] K. M. Schultz, K. A. Kyburz, K. S. Anseth, *Proc. Natl. Acad. Sci. USA* **2015**, *112*, E3757.
[134] O. Chaudhuri, L. Gu, M. Darnell, D. Klumpers, S. A. Bencherif, J. C. Weaver, N. Huebsch, D. J. Mooney, *Nat. Commun.* **2015**, *6*, 6364.
[135] T. L. Sun, T. Kurokawa, S. Kuroda, A. B. Ihsan, T. Akasaki, K. Sato, M. A. Haque, T. Nakajima, J. P. Gong, *Nat. Mater.* **2013**, *12*, 932.
[136] C. W. Peak, J. J. Wilker, G. Schmidt, *Colloid Polym. Sci.* **2013**, *291*, 2031.
[137] R. Du, J. Wu, L. Chen, H. Huang, X. Zhang, J. Zhang, *Small* **2014**, *10*, 1387.
[138] H. P. Cong, P. Wang, S. H. Yu, *Small* **2014**, *10*, 448.
[139] T. Wang, S. Zheng, W. Sun, X. Liu, S. Fu, Z. Tong, *Soft Matter* **2014**, *10*, 3506.
[140] K. H. Vining, D. J. Mooney, *Nat. Rev. Mol. Cell Biol.* **2017**, *18*, 728.
[141] W. J. Hadden, J. L. Young, A. W. Holle, M. L. McFetridge, D. Y. Kim, P. Wijesinghe, H. Taylor-Weiner, J. H. Wen, A. R. Lee, K. Bieback, B. N. Vo, D. D. Sampson, B. F. Kennedy, J. P. Spatz, A. J. Engler, Y. S. Choi, *Proc. Natl. Acad. Sci. USA* **2017**, *114*, 5647.
[142] P. C. D. P. Dingal, A. M. Bradshaw, S. Cho, M. Raab, A. Buxboim, J. Swift, D. E. Discher, *Nat. Mater.* **2015**, *14*, 951.
[143] C. Yang, M. W. Tibbitt, L. Basta, K. S. Anseth, *Nat. Mater.* **2014**, *13*, 645.
[144] C. X. Li, N. P. Talele, S. Boo, A. Koehler, E. Knee-Walden, J. L. Balestrini, P. Speight, A. Kapus, B. Hinz, *Nat. Mater.* **2017**, *16*, 379.
[145] Z. Gong, S. E. Szczesny, S. R. Caliari, E. E. Charrier, O. Chaudhuri, X. Cao, Y. Lin, R. L. Mauck, P. A. Janmey, J. A. Burdick, V. B. Shenoy, *Proc. Natl. Acad. Sci. USA* **2018**, *115*, E2686.
[146] E. E. Charrier, K. Pogoda, R. G. Wells, P. A. Janmey, *Nat. Commun.* **2018**, *9*, 449.
[147] J. Lou, R. Stowers, S. Nam, Y. Xia, O. Chaudhuri, *Biomaterials* **2018**, *154*, 213.
[148] O. Chaudhuri, L. Gu, D. Klumpers, M. Darnell, S. A. Bencherif, J. C. Weaver, N. Huebsch, H. P. Lee, E. Lippens, G. N. Duda, D. J. Mooney, *Nat. Mater.* **2016**, *15*, 326.
[149] N. Bonakdar, R. Gerum, M. Kuhn, M. Sporrer, A. Lippert, W. Schneider, K. E. Aifantis, B. Fabry, *Nat. Mater.* **2016**, *15*, 1090.
[150] S. Nam, J. Lee, D. G. Brownfield, O. Chaudhuri, *Biophys. J.* **2016**, *111*, 2296.
[151] C. M. Madl, B. L. LeSavage, R. E. Dewi, C. B. Dinh, R. S. Stowers, M. Khariton, K. J. Lampe, D. Nguyen, O. Chaudhuri, A. Enejder, S. C. Heilshorn, *Nat. Mater.* **2017**, *16*, 1233.
[152] B. D. Cosgrove, K. L. Mui, T. P. Driscoll, S. R. Caliari, K. D. Mehta, R. K. Assoian, J. A. Burdick, R. L. Mauck, *Nat. Mater.* **2016**, *15*, 1297.
[153] J. E. Samorezov, C. M. Morlock, E. Alsberg, *Bioconjugate Chem.* **2015**, *26*, 1339.
[154] C. Yang, F. W. DelRio, H. Ma, A. R. Killaars, L. P. Basta, K. A. Kyburz, K. S. Anseth, *Proc. Natl. Acad. Sci. USA* **2016**, *113*, E4439.
[155] C. H. R. Kuo, J. Xian, J. D. Brenton, K. Franze, E. Sivaniah, *Adv. Mater.* **2012**, *24*, 6059.
[156] S. S. Rao, S. Bentil, J. DeJesus, J. Larison, A. Hissong, R. Dupaix, A. Sarkar, J. O. Winter, *PLoS One* **2012**, *7*, e35852.
[157] K. Chatterjee, S. Lin-Gibson, W. E. Wallace, S. H. Parekh, Y. J. Lee, M. T. Cicerone, M. F. Young, C. G. Simon, *Biomaterials* **2010**, *31*, 5051.
[158] J. K. Choi, P. Agarwal, H. Huang, S. Zhao, X. He, *Biomaterials* **2014**, *35*, 5122.
[159] H. Y. Liu, T. Greene, T. Y. Lin, C. S. Dawes, M. Korc, C. C. Lin, *Acta Biomater.* **2017**, *48*, 258.
[160] M. L. Previtera, K. L. Trout, D. Verma, U. Chippada, R. S. Schloss, N. A. Langrana, *Ann. Biomed. Eng.* **2012**, *40*, 1061.
[161] H. Shih, C. C. Lin, *J. Mater. Chem. B* **2016**, *4*, 4969.
[162] H. Y. Yoshikawa, F. F. Rossetti, S. Kaufmann, T. Kaindl, J. Madsen, U. Engel, A. L. Lewis, S. P. Armes, M. Tanaka, *J. Am. Chem. Soc.* **2011**, *133*, 1367.
[163] S. Hackelbusch, T. Rossow, D. Steinhilber, D. A. Weitz, S. Seiffert, *Adv. Healthcare Mater.* **2015**, *4*, 1841.
[164] S. Tang, M. J. Glassman, S. Li, S. Socrate, B. D. Olsen, *Macromolecules* **2014**, *47*, 791.
[165] N. Kong, Q. Peng, H. Li, *Adv. Funct. Mater.* **2014**, *24*, 7310.
[166] W. Yuan, J. Yang, P. Kopeckova, J. Kopecek, *J. Am. Chem. Soc.* **2008**, *130*, 15760.
[167] H. Liu, J. Usprech, Y. Sun, C. A. Simmons, *Acta Biomater.* **2016**, *34*, 113.
[168] L. Wang, Y. Li, B. Chen, S. Liu, M. Li, L. Zheng, P. Wang, T. J. Lu, F. Xu, *ACS Appl. Mater. Interfaces* **2015**, *7*, 15088.
[169] H. Y. Hsieh, G. Camci-Unal, T.-W. Huang, R. Liao, T. J. Chen, A. Paul, F. G. Tseng, A. Khademhosseini, *Lab Chip* **2014**, *14*, 482.
[170] L. Bian, J. V. Fong, E. G. Lima, A. M. Stoker, G. A. Ateshian, J. L. Cook, C. T. Hung, *Tissue Eng., Part A* **2010**, *16*, 1781.
[171] T. Guo, L. Yu, C. G. Lim, A. S. Goodley, X. Xiao, J. K. Placone, K. M. Ferlin, B. N. B. Nguyen, A. H. Hsieh, J. P. Fisher, *Ann. Biomed. Eng.* **2015**, *44*, 2103.
[172] R. Tamate, T. Ueki, Y. Kitazawa, M. Kuzunuki, M. Watanabe, A. M. Akimoto, R. Yoshida, *Chem. Mater.* **2016**, *28*, 6401.
[173] D. D. McKinnon, D. W. Domaille, J. N. Cha, K. S. Anseth, *Adv. Mater.* **2014**, *26*, 865.
[174] C. T. S. W. P. Foo, J. S. Lee, W. Mulyasasmita, A. Parisi-Amon, S. C. Heilshorn, *Proc. Natl. Acad. Sci. USA* **2009**, *106*, 22067.
[175] F. Ito, K. Usui, D. Kawahara, A. Suenaga, T. Maki, S. Kidoaki, H. Suzuki, M. Taiji, M. Itoh, Y. Hayashizaki, T. Matsuda, *Biomaterials* **2010**, *31*, 58.
[176] K. Ye, X. Wang, L. P. Cao, S. Y. Li, Z. H. Li, L. Yu, J. D. Ding, *Nano Lett.* **2015**, *15*, 4720.
[177] K. Ye, L. P. Cao, S. Y. Li, L. Yu, J. D. Ding, *ACS Appl. Mater. Interfaces* **2016**, *8*, 21903.
[178] T. A. Ulrich, E. M. de Juan Pardo, S. Kumar, *Cancer Res.* **2009**, *69*, 4167.
[179] D. E. Ingber, *Int. J. Dev. Biol.* **2006**, *50*, 255.
[180] A. P. Sage, Y. Tintut, L. L. Demer, *Nat. Rev. Cardiol.* **2010**, *7*, 528.
[181] M. Whang, J. Kim, *Tissue Eng. Regener. Med.* **2016**, *13*, 126.
[182] A. D. Rape, M. Zibinsky, N. Murthy, S. Kumar, *Nat. Commun.* **2015**, *6*, 8129.
[183] S. Nemir, H. N. Hayenga, J. L. West, *Biotechnol. Bioeng.* **2010**, *105*, 636.
[184] C. Colosi, S. R. Shin, V. Manoharan, S. Massa, M. Costantini, A. Barbetta, M. R. Dokmeci, M. Dentini, A. Khademhosseini, *Adv. Mater.* **2016**, *28*, 677.
[185] W. J. Polacheck, R. Li, S. G. Uzel, R. D. Kamm, *Lab Chip* **2013**, *13*, 2252.
[186] G. D. Nicodemus, S. J. Bryant, *Tissue Eng., Part B* **2008**, *14*, 149.
[187] K. A. Jansen, R. G. Bacabac, I. K. Piechocka, G. H. Koenderink, *Biophys. J.* **2013**, *105*, 2240.
[188] P. C. Georges, J. J. Hui, Z. Gombos, M. E. McCormick, A. Y. Wang, M. Uemura, R. Mick, P. A. Janmey, E. E. Furth, R. G. Wells, *Am. J. Physiol.: Gastrointest. Liver Physiol.* **2007**, *293*, G1147.
[189] I. Acerbi, L. Cassereau, I. Dean, Q. Shi, A. Au, C. Park, Y. Chen, J. Liphardt, E. Hwang, V. Weaver, *Integr. Biol.* **2015**, *7*, 1120.
[190] B. D. Riehl, J.-H. Park, I. K. Kwon, J. Y. Lim, *Tissue Eng., Part B* **2012**, *18*, 288.

[191] J. A. Pedersen, M. A. Swartz, *Ann. Biomed. Eng.* **2005**, *33*, 1469.
[192] H. Liu, Y. Sun, C. A. Simmons, *J. Biomech.* **2013**, *46*, 1967.
[193] L. Bian, D. Y. Zhai, E. C. Zhang, R. L. Mauck, J. A. Burdick, *Tissue Eng., Part A* **2011**, *18*, 715.
[194] M. H. van Marion, N. A. Bax, M. C. van Turnhout, A. Mauretti, D. W. van der Schaft, M. J. T. Goumans, C. V. Bouten, *J. Mol. Cell. Cardiol.* **2015**, *87*, 79.
[195] P. H. Kouwer, M. Koepf, V. A. Le Sage, M. Jaspers, A. M. van Buul, Z. H. Eksteen-Akeroyd, T. Woltinge, E. Schwartz, H. J. Kitto, R. Hoogenboom, *Nature* **2013**, *493*, 651.
[196] M. Geerligs, G. W. M. Peters, P. A. J. Ackermans, C. W. J. Oomens, F. P. T. Baaijens, *Biorheology* **2008**, *45*, 677.
[197] I. Levental, P. C. Georges, P. A. Janmey, *Soft Matter* **2007**, *3*, 299.
[198] Z. Liu, L. E. Bilston, *Biorheology* **2000**, *37*, 191.
[199] C. D. Katsetos, M. M. Herman, S. J. Mörk, *Cell Motil. Cytoskeleton* **2003**, *55*, 77.
[200] L. F. Eng, R. S. Ghirnikar, Y. L. Lee, *Neurochem. Res.* **2000**, *25*, 1439.
[201] L. Dehmelt, S. Halpain, *Genome Biol.* **2004**, *6*, 204.
[202] M. M. Black, V. Lee, *J. Neurosci.* **1988**, *8*, 3296.
[203] S. S. Scherer, P. E. Braun, J. Grinspan, E. Collarini, D. Y. Wang, J. Kamholz, *Neuron* **1994**, *12*, 1363.
[204] N. J. Steinmetz, S. J. Bryant, *Biotechnol. Bioeng.* **2012**, *109*, 2671.
[205] M. S. Rehmann, J. I. Luna, E. Maverakis, A. M. Kloxin, *J. Biomed. Mater. Res., Part A* **2016**, *104*, 1162.
[206] P. J. Yang, M. E. Levenston, J. S. Temenoff, *Tissue Eng., Part A* **2012**, *18*, 2365.
[207] A. Ranga, N. Gjorevski, M. P. Lutolf, *Adv. Drug Delivery Rev.* **2014**, *69*, 19.
[208] A. L. Bredenoord, H. Clevers, J. A. Knoblich, *Science* **2017**, *355*, eaaf9414.
[209] J. I. Lopez, I. Kang, W. K. You, D. M. McDonald, V. M. Weaver, *Integr. Biol.* **2011**, *3*, 910.
[210] N. Gjorevski, A. Ranga, M. P. Lutolf, *Development* **2014**, *141*, 1794.
[211] R. Hiramatsu, T. Matsuoka, C. Kimura-Yoshida, S. W. Han, K. Mochida, T. Adachi, S. Takayama, I. Matsuo, *Dev. Cell* **2013**, *27*, 131.
[212] Y. Sasai, M. Eiraku, H. Suga, *Development* **2012**, *139*, 4111.
[213] Y. F. Li, K. A. Kilian, *Adv. Healthcare Mater.* **2015**, *4*, 2780.
[214] U. A. Gurkan, R. El Assal, S. E. Yildiz, Y. Sung, A. J. Trachtenberg, W. P. Kuo, U. Demirci, *Mol. Pharm.* **2014**, *11*, 2151.
[215] O. Jeon, E. Alsberg, *Adv. Funct. Mater.* **2013**, *23*, 4765.
[216] U. A. Gurkan, Y. Sung, R. El Assal, F. Xu, A. Trachtenberg, W. Kuo, U. Demirci, *J. Tissue Eng. Regener. Med.* **2012**, *6*, 366.
[217] S. Tasoglu, U. Demirci, *Trends Biotechnol.* **2013**, *31*, 10.
[218] B. Gao, Q. Yang, X. Zhao, G. Jin, Y. Ma, F. Xu, *Trends Biotechnol.* **2016**, *34*, 746.
[219] H. Onoe, M. Kato-Negishi, A. Itou, S. Takeuchi, *Adv. Healthcare Mater.* **2016**, *5*, 1104.
[220] X. W. Bao, Z. Y. Li, H. Liu, K. Feng, F. C. Yin, H. J. Li, J. H. Qin, *Mol. Med. Rep.* **2018**, *17*, 2277.
[221] S. Sart, S. N. Agathos, Y. Li, T. Ma, *Biotech. J.* **2016**, *11*, 43.
[222] H. Y. Wang, S. C. Heilshorn, *Adv. Mater.* **2015**, *27*, 3717.
[223] A. Higuchi, Q. D. Ling, S. S. Kumar, Y. Chang, T. C. Kao, M. A. Munusamy, A. A. Alarfaj, S. T. Hsu, A. Umezawa, *Prog. Polym. Sci.* **2014**, *39*, 1585.
[224] B. Cheng, M. Lin, Y. H. Li, G. Y. Huang, H. Yang, G. M. Genin, V. S. Deshpande, T. J. Lu, F. Xu, *Biophys. J.* **2016**, *111*, 2051.
[225] J. A. Fallas, J. D. Hartgerink, *Nat. Commun.* **2012**, *3*, 1087.
[226] Y. Ma, Y. Ji, M. You, S. Wang, Y. Dong, G. Jin, M. Lin, Q. Wang, A. Li, X. Zhang, *Acta Biomater.* **2016**, *42*, 199.
[227] B. R. Smith, S. S. Gambhir, *Chem. Rev.* **2017**, *117*, 901.
[228] E. A. Sander, T. Stylianopoulos, R. T. Tranquillo, V. H. Barocas, *Proc. Natl. Acad. Sci. USA* **2009**, *106*, 17675.
[229] B. Chen, B. H. Ji, H. J. Gao, *Ann. Rev. Biophys.* **2015**, *44*, 1.
[230] S. Ansari, P. Sarrion, M. M. Hasani-Sadrabadi, T. Aghaloo, B. M. Wu, A. Moshaverinia, *J. Biomed. Mater. Res., Part A* **2017**, *105*, 2957.
[231] J. A. Yang, J. Yeom, B. W. Hwang, A. S. Hoffman, S. K. Hahn, *Prog. Polym. Sci.* **2014**, *39*, 1973.
[232] D. Srivastava, N. DeWitt, *Cell* **2016**, *166*, 1386.